University of South Bohemia

Faculty of Science

Differential gene expression as a tool to sort individual life stages of a mammalian parasite *Trypanosoma brucei*

Master thesis

Bc. Michaela Kunzová

Supervisor: RNDr. Alena Panicucci Zíková, Ph.D.

Co-supervisor: Mgr. Eva Doleželová, Ph.D.

České Budějovice 2018

Kunzová M, 2018, Differential gene expression as a tool to sort individual life stages of a mammalian parasite *Trypanosoma brucei* Mgr Thesis, in English – 53 p., Faculty of Science, University of South Bohemia, České Budějovice, Czech Republic

Annotation:

This master thesis aimed to develop a system to sort individual life cycle stages of the mammalian parasite *Trypanosoma brucei* generated *in vitro*. *T. brucei* cell lines expressing developmentally regulatable fluorescent protein due to the stage specific 3'UTRs were generated. Furthermore, a double knock-out of a protein (TbIF1) presumably involved in the parasite's differentiation was attempted.

I hereby declare that I worked on this master thesis on my own and used only the resources mentioned in the bibliography.

I hereby declare that, in accordance with Article 47b of Act No. 111/1998 in the valid wording, I agree with the publication of my master thesis, in full to be kept in the Faculty of Science archive, in electronic form in publicly accessible part of the STAG database operated by the University of South Bohemia in České Budějovice accessible through its web pages.

Further, I agree to the electronic publication of the comments of my supervisor and thesis opponents and the record of the proceedings and results of the thesis defence in accordance with aforementioned Act No. 111/1998. I also agree to the comparison of the text of my thesis with the Theses.cz thesis database operated by the National Registry of University Theses and a plagiarism detection system.

Date.....

Signature.....

Acknowledgement:

Firstly, I would like to thank from the bottom of my heart my supervisor Dr. Alena Paniccuci Zíková for allowing me to be a part of her amazing team. Next, I would like to express my deepest gratitude towards my co-supervisor Dr. Eva Doleželová. Both had incredible patience with me during my master studies. Furthermore, I want to thank all wonderful people from AZ lab, as they were always ready to help me or to cheer me up. Brian, Ondra, Carol, Geri, Minal and Simona, you are amazing! Thank you! I owe you a non-alcoholic drink! Next, I would like to thank to Lukas and Kachna. You made me laugh, when I wanted to cry and showed me, how a simple day can be beautiful. Finally, I would like to thank my friends and family for their support.

Table of content

1. Introduction

1.1. *Trypanosoma brucei* as a model to study mitochondrion remodelling

Trypanosoma brucei is a unicellular organism, which phylogenetically belongs to a highly diverged branch of the eukaryotic tree called Kinetoplastida. The genera *Trypanosoma* consists of mammalian parasites causing important infectious diseases of humans and livestock. The most well-known diseases caused by *T. brucei* are Human and Animal African Trypanosomiases. Although *T. brucei* was in the past studied mainly because of its detrimental burden on human population in the developing world, this organism has gained its rightful place besides other model organisms, e.g. *Drosophila melanogaster*, *Saccharomyces cerevisiae*, *Mus musculus*, *Ceanorhabditis elegans* and others, as it is amenable to forward and reverse genetics methods. Moreover, its cell possesses many unique and interesting features of cellular biology. One of them is the ability of the parasite to change morphology, gene expression and metabolism during its complex life cycle when it encounters vastly different environments.

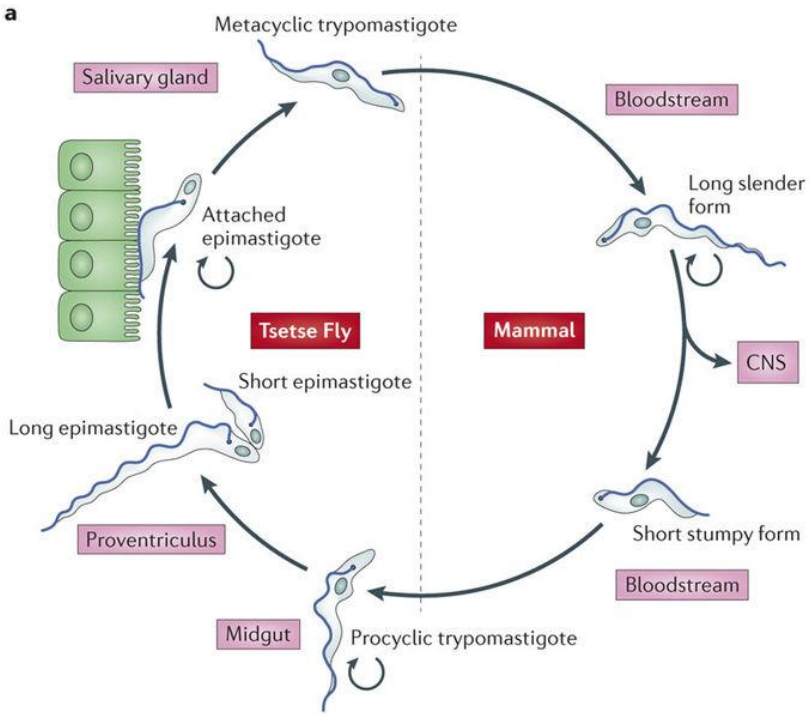

Figure 1: Trypanosoma brucei simplified life cycle (Langousis and Hill, 2014).

Simplified life cycle of *T. brucei* is shown in Figure 1. This parasite alternates between two hosts – a mammal and a tsetse fly. The latter serves as a vector and enables

the spreading of the parasite from one mammalian host to another. The tsetse fly ingests transmission-ready bloodstream stumpy form during the bloodmeal on an infected mammalian host. Once in the tsetse fly, the stumpy form parasite transforms into the proliferative procyclic trypomastigote form (PF) (Figure 1) (reviewed in Dyer et al, 2013 and Sharma et al, 2009). This stage then migrates to the proventriculus, where it differentiates via asymmetric division into long and short epimastigotes. Epimastigote form is defined by a different position of its mitochondrial genome called kinetoplast relatively to the nucleus, as it is placed anteriorly to it (Vickerman, 1988). The position of the kinetoplast changes back to the posterior end when the short epimastigote form reaches salivary glands. Additionally, the epimastigote form attaches itself to the epithelium and undergoes another asymmetrical division resulting in one premetacyclic cell and one short epimastigote cell. The premetacyclic cell subsequently differentiates into a metacyclic cell through a process which is not fully understood yet (Rotureau et al, 2012). The metacyclic form is the first infective stage for the mammalian host. Once in the host, the metacyclic trypanosomes differentiate into long slender bloodstream forms (BF). This life stage establishes and maintains the infection in the host´s bloodstream. Eventually, the central nervous system is invaded by these parasites causing the lethal symptoms of the disease. However, in order to close the life cycle, the BF cells transform to short stumpy forms, which are transmitted to the tsetse fly during its bloodmeal. (reviewed in Langousis and Hill, 2014)

One of the most prominent changes happening during the *T. brucei* life cycle occurs in the parasite single mitochondrion. While in the BF the mitochondrion forms a simple tubular structure stretching just from the anterior to the posterior end of the cell with no detectable cristae, the PF mitochondrion is highly branched throughout the whole cell with fully developed cristae. In addition to these major morphological changes, the mitochondrial metabolism alters as well. The glucose rich environment of the mammalian bloodstream ensures a high income of adenosine triphosphate (ATP) for BF cells by highly active glycolysis. In this form, the mitochondrion is not the main ATP provider, but remains the niche for other important cellular processes (e.g. maintaining mitochondrial membrane potential, Ca2+ homeostasis, acetate production, FeS cluster synthesis etc.) (Roldán et al, 2011; Mazet et al, 2013; Basu et al, 2016). Interestingly, the canonical cytochrome-mediated respiratory chain is missing in the BF cells and the essential mitochondrial membrane potential is generated by ATP-hydrolytic activity of the FoF1 ATPase, a proton pump that transport protons across the mitochondrial inner membrane at the expense of ATP.

The respiration occurs independently through a plant-like alternative oxidase (AOX or TAO). (reviewed in Smith et al, 2017)

On the other hand, the PF cells face a completely different environment in the arthropod vector with ultimately no glucose present. Thus, the parasite depends mainly on amino acids (e.g. L-proline) as their energy source and employs oxidative phosphorylation (OXPHOS) for their ATP production (reviewed in Smith et al, 2017). OXPHOS pathway takes place on the inner mitochondrial membrane and it is fully dependent on the canonical electron transport chain (ETC) complexes I, III and IV as they pump protons across the inner membrane. This proton gradient is then utilized by ATP-generating complex, FoF1 ATPase (Mitchell, 1961). How the parasite´s mitochondrion switches from the ATP-producing to ATP-consuming organelle is not unravelled yet. However, similar metabolic rewiring happens in the cancer cells when these cells undergo so called Warburg effect and switch to aerobic glycolysis for their ATP production. As a result of intensive studies, a few possible candidates responsible for this metabolic remodelling have been identified.

One of the candidates is a small peptide called Inhibition Factor 1 (IF1). This protein is a eukaryotic invention as the corresponding gene was identified only in the genomes of eukaryotic organisms (Pullman and Monroy, 1963). The exact role of this protein in the mitochondria is not fully understood yet, but this peptide was originally identified as an inhibitor of the hydrolytic activity of the FoF1 ATPase presumably to protect cells from ATP depletion under ischemic conditions (Campanella et al, 2008). Since then, additional roles (e.g. trigger of mild reactive oxygen species (ROS) production, activator of NFκB pathway, signal for cell pro-survival and proliferative decision, etc.) were attributed to this protein. Importantly, IF1 seems to be overexpressed in several cancer cell lines (lung, ovary, breast, colon), neurones and hepatocytes. Its induced overexpression causes increased levels of ROS which can signal cell proliferation, invasion and support cell survival (reviewed in García-Bermúdez and Cuezva, 2016). Recently, our laboratory has identified the homologues protein, TbIF1 (Tb927.10.2970), in *Trypanosoma brucei* genome (Panicucci et al, 2017). Since there is a possible analogy between the *T. brucei* and cancer cells metabolic rewiring it would be worth to examine the role of TbIF1 during the *T. brucei* cells differentiation.

The second candidate molecules, which may play important role in cell differentiation, are ROS. ROS comprise of molecules (e.g. H_2O_2, $O_2^{\cdot -}$, NO etc), which are mainly known as deleterious molecules and by-products of active aerobic electron transport chain. Nonetheless, available data from plants and bacteria suggest that these molecules function as signals to alter gene expression or metabolic response. For example, there have been reports showing that in mammalian cells upon a certain external stimulus, ROS levels were elevated and similarly, these cells did not react to the same stimuli if the ROS generating pathways were blocked (reviewed in Rhee, 1999). Interestingly, introduction of catalase, a ROS scavenger, into the genome of catalase-lacking *Trypanosoma cruzi* impaired the ROS production and thus the cell signalling under oxidative stress conditions (Freire et al, 2017). The hypothesis that ROS molecules may play important roles during *T. brucei* differentiation is supported by our preliminary data showing elevated ROS levels in epimastigotes (Doleželová et al., unpublished data).

The individual life cycle stages and the transition from midgut procylic trypomastigotes to metacyclics were characterized using infected tsetse flies from which the different life cycle forms were dissected. However, this approach is time consuming and skill-demanding. At the same it provides only a small number of parasites to examine. For this reason, there has been a search for a methodology, how to mimic *in vivo* differentiation *in vitro*. While cis-aconitate with the combination of lowered temperature have been used to trigger the transition from BF to PF *in vitro* for decades (Czichos et al, 1986), the *in vitro* transition from PF to metacyclics has been established just recently (Kolev et al, 2012).

In 2012, Kolev et al published a ground-breaking paper presenting an artificial system in which the transition from PF to BF is triggered by overexpression of RNA binding protein 6 (RBP6) (Kolev et al, 2012). After two days of induced RBP6 overexpression, epimastigote-like cells formed in the culture; three days later metacyclic-like cells appeared. These cells possess typical metacyclic cell features as: undulating membrane, active endocytosis, posterior position of the kinetoplast, no adhesion to glass, bloodstream like motility, mitochondrial regression and higher expression levels of calflagins – a BF protein marker. Most importantly, these cells once injected into the mouse model were able to establish infection.

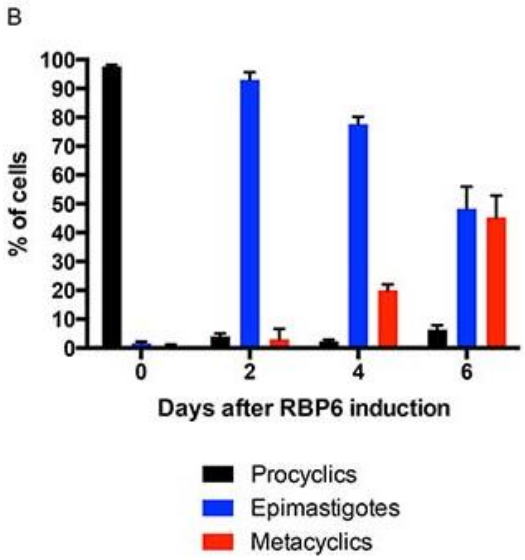

Figure 2: The cell in vitro *differentiation by inducible overexpression of RBP6 protein in SDM-80 media (without glucose) (Doleželová et al, unpublished data).*

Fascinated by this system, we have introduced the *in vitro* differentiation in our laboratory. Figure 2 shows our data which are in full agreement with the published observation (Kolev et al, 2012). The differentiation is a little bit faster as the cells are cultured in the medium without glucose. *T. brucei* culture at day 0 consists only of procyclic life forms. At day 2, the culture contains mainly epimastigote cells, with only a small number of procyclic cells. Two days later, at day 4, about 20 % of the cells are in metacyclic form, at day 6 metacyclic form represents approximately 45 % of the cells, epimastogotes are still present at approximately 50 % are epimastigote, with the remaining cells being classified as procyclic forms.

This artificial system is an extremely helpful tool to study trypanosome insect-life stages by producing these different cellular forms in sufficient quantities to perform various biochemical analyses. Nonetheless, the mixed character of the culture (presence of different life cycle stages at the same time) possesses a disadvantage to this system. Thus, the need to sort individual life stages from the culture emerges.

To fulfil this goal, a few different approaches can be possible: i) use of life stage-specific surface protein molecules which can be targeted by specific antibodies labelled with a fluorescent marker; ii) use of proteins which are exclusively expressed in the individual life stages and endogenously tag these proteins with green fluorescent protein (GFP) or its modifications; iii) use 3´untranslated regions (3´UTRs) of specific genes, which

are strictly regulated during the life cycle of the parasite. The last strategy is possible due to unique regulation of gene expression in *T. brucei* compared to the conventional model organisms. The following chapter summarizes the basic knowledge on this topic.

1.2. Trypanosoma gene expression during its life cycle

In canonical eukaryotic system, the regulation of gene expression happens mainly at the transcriptional levels. In contrast, *T. brucei* transcribes its genes in long polycistronic units that contain genes of independent and different functions. Thus, it is widely accepted that the regulation of gene expression in *T. brucei* occurs at the post-transcriptional level (reviewed in Preußer et al, 2012) mainly at the level of mRNA stability, which is regulated by trans-acting elements to its 3'UTR (Jefferies et al, 1991; Furger et al, 1997).

So far, several stage specific proteins were already identified (Wurst et al, 2012; Urwyler et al, 2007). Generally, these proteins are expressed at the Trypanosoma surface coat and thus they can be detected by antibodies. The surface coat differs significantly between the PF and BF cells. While the PF surface coat is made of mainly proteins called procyclins (Roditi, 1987), the surface coat of the metacyclics and BF cells contains variable surface glycoproteins (VSGs). Although it should be noted that metacyclics possess a specific and noticeably smaller set of VSG proteins compared to BFs (Crowe et al, 1983). Interestingly, the BF cells use synchronized replacement of the VSGs as a mean to evade the mammalian immune system by process called antigenic variation (Cross, 1975). The epimastigote life stage has brucei alanine rich proteins (BARP) embedder in their surface coat (Urwyler et al, 2007). Another gene candidate, which is expressed only in the metacyclics and BF cells, is RNA binding protein 10 (RBP10) (Wurst et al, 2012). RBP10 belongs together with RBP6 to a family of RNA binding proteins which function as a key regulator switches during the life cycle (reviewed in Kolev et al, 2014). Both proteins recognize specific motifs on mRNAs and target the mRNA for translation repression. For example, RBP10 interacts with procyclin and cytochrome c oxidase subunits mRNAs and targets them for a quick destabilization in the BF parasites (Mugo et al, 2017). The significance of this regulation is exemplified by the fact, that RBP10 is essential for BF cells survival (Wurst et al, 2012).

Based on available information showing that 3´UTRs can be the sole or at least the main regulator of mRNA expression, we hypothesized that 3´UTRs of specific genes

might be used to regulate expression of the marker protein (e.g. GFP). Therefore, in this thesis we explored our hypothesis by tagging a fluorescent protein with 3'UTR of a stage specific gene and followed the expression of the fluorescent protein during the *T. brucei* differentiation *in vitro*. Furthermore, I was involved in generation of TbIF1 double knock-out cell line, which will be used in future studies to determine the putative role of TbIF1 during the *T. brucei* differentiation.

2. Aims

- to identify 3‘UTR regions of differentially expressed genes during *T. brucei* differentiation *in vitro*
- to generate constructs containing fluorescent proteins fused to these 3‘UTRs
- to generate *T. brucei* strains that will express fluorescent protein in specific life cycle stages
- to perform double knock-out of TbIF1

3. Methods

3.1. *T. brucei* cell lines

Trypanosoma brucei brucei procyclic form (Lister 427 strain) was used in all our experiments as a wild type (wt) strain. The RBP6 overexpression cell line is derived from 29-13 cell line (Wirtz et al, 1999) by insertion of pLew100-RBP6-Phleo linearized plasmid to rRNA spacer. The RBP6 overexpression is triggered by adding of tetracycline (1-10μg/ml) into the medium. The PF cells were cultivated at 27°C in three different media: i) the glucose containing SDM-79 with dialyzed 10% FBS (Fetal bovine serum), ii) the glucose-lacking SDM-80 with dialyzed 10% FBS and 50mM N-acetyl glucosamine (Sigma-Aldrich®), and iii) conditional media prepared by mixing 50% SDM-80 media and 50% of supernatant of SDM-79 media in which wt cells were grown for 48 hours.

3.2. Primer design and polymerase chain reaction (PCR) to amplify 3'UTRs of RBP10 and BARP gene

The 3'UTR of RBP10 (Tb927.8.2780) gene is well defined in the TriTrypDB, an integral genomic and functional genomic database for pathogens of the family Trypanosomatidae. However, BARPs are encoded by 14 different genes and their 3'UTRs differ significantly. Based on obtained transcriptomic data, we chose the 3'UTR of BARP_15610 gene (Tb927.9.15610).

The forward primers were designed to contain XhoI restriction site while the reverse primers contain KpnI restriction site in order to facilitate the cloning (Table I).

Table I: Primers used to amplify 3'UTR of RBP10 and BARP_15610. Underlined letters correspond with the inserted restriction site. Sequences are shown from 5'→3' direction.

Primer	Code name	Restriction site	Sequence
RBP10 3'UTR Fw	AZ0829	XhoI	CAGCTCGAGTGGCACAGAGGGTAAC
RBP10 3'UTR Rv	AZ0830	KpnI	CATGGTACCCAACTAAAAGTAACGGTGATGGG
BARP_15610 3'UTR Fw	AZ0806	XhoI	CACCTCGAGGAGGTTGCAACTCCATG
BARP_15610 3'UTR Rv	AZ0828	KpnI	CTAGGTACCCATGATAAAATAAAACCCCTCAG

To amplify the region defined by designed primers, the PCR with Taq polymerase was used. Since this enzyme adds an additional base "A" at the end of the amplified sequence, the PCR product was directly ligated into pGEM®-T Easy vector (Promega), a high copy number plasmid with multiple cloning site (MCS) present within the lacZ sequence allowing a blue-white selection.

Table II: The composition of PCR mix for amplification of BARP_15610 3'UTR and RBP10 3'UTR.

Solution	Volume
10x Blue Buffer complete	5µl
Genomic DNA (200ng)	1µl
10mM dNTP mix	1µl
Fw primer (10µM)	2.5µl
Rv primer (10µM)	2.5µl
Taq-Purple polymerase (1U/µl)	2.5µl
MilliQ water	35.5µl

Since the calculated annealing temperatures were almost identical for all four primers, the same PCR conditions were used to amplify both products, the 501 base pairs (bp) long 3'UTR of BARP_15610 and the 1094bp long 3'UTR of RBP10 (Table III).

Table III: The PCR condition for the amplification of RBP10 3'UTR and BARP 3'UTR.

Segment	Cycles	Temperature	Time
1	1	94°C	2 minutes
2	35	94°C	30 seconds
		50°C	30 seconds
		72°C	1 minute
3	1	72°C	7 minutes

PCR products were then separated on 1% agarose gel in electrophoresis apparatus. Subsequently, the bands of corresponding size were excised and gel purified by commercially available kit (GenElute™ Gel Extraction Kit, Sigma-Aldrich®).

3.3. Ligation of either RBP10 or BARP_15610 into pGEM-T easy plasmid and subsequent transformation into *E. coli*

Purified DNA fragments amplified by PCR were subsequently ligated into the pGEM®-T Easy vector. This vector was chosen based on its ability to determine positive colonies by so called blue-white screening.

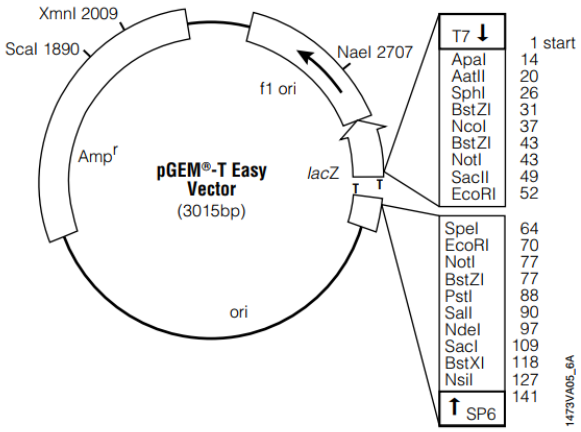

Figure 3: The map of pGEM®-T Easy vector used for blue-white screening (Promega, Technical manual pGEM®-T and pGEM®-T Easy Vector Systems).

The blue-white screening is based on disruption of the β-galactosidase gene (lacZ) by the inserted PCR product. Within the lacZ coding region there is a MCS containing several restriction sites in addition to "T" overhangs, which are used to insert the sequence of interest (Figure 3). This insertional inactivation of the LacZ is detected by the change in colour of X-gal (5-Bromo-4-Chloro-3-Indolyl β-D-Galactopyranoside) on an agar plate. Since the functional β-galactosidase cleaves X-gal, the colonies containing plasmid with no inserted DNA appear blue, while the colonies containing plasmid with the inserted DNA are white (i.e. the β-galactosidase enzyme is not functional (Promega, Technical manual pGEM®-T and pGEM®-T Easy Vector Systems)).

Firstly, the ligation reaction was set up, to attach our fragments into the pGEM-T easy vector. The 10µl ligation reaction contained insert DNA (3´UTR for either BARP_15610 or RBP10) and vector (pGEM-T easy) in ratio of 3:1, 1µl of T4 ligase (1U/µl) and 1µl of 10x ligase buffer. This reaction mix was incubated at 4°C overnight.

Then the ligation mixtures were transformed into *Escherichia coli* XL1-blue competent cells. Freshly thawed competent cells (60µl) were mixed with ligation mix (6µl) and incubated on ice for 15 minutes. After that, the cells were heat-shocked at 42°C for 50 seconds. Immediately after the heat shock, the cells were placed on ice for 2 minutes. Subsequently, 400µl of S.O.C media were added and the mixture was shaken at 200rpm at 37°C for 1 hour. Consequently, the transformed cells were spread on an agar plate with the selective antibiotic – in our case ampicillin (100µg/ml). The agar plates were placed to 37°C incubator and left overnight.

The white colonies were selected and grown in LB media overnight and pGEM-T easy plasmids were extracted by commercially available kit (GenElute™ Plasmid Miniprep Kit, Sigma-Aldrich®). Purified plasmids were digested with restriction enzymes XhoI and KpnI (1 hour, 37°C) and separated by DNA electrophoresis to verify the cloning. One selected clone with correct restriction pattern was sequenced to confirm the identity of the inserted fragment (sequencing done by Seqme s.r.o.).

3.4. Generation of pHD1344 plasmids containing fluorescent proteins mNeonGreen and tdTomato joined to 3'UTR of either BARP_15610 or RBP10

The different distinct life cycle stages will be monitored by a fluorescence marker protein, which expression is regulated by the 3´UTR of RBP10 or BARP_15610 gene. In order to have two fluorescent markers of different emission wavelength in one cell line we chose to use mNeonGreen (excitation maximum at 506nm, emission maximum at 517nm) (http://www.allelebiotech.com/mneongreen/) and tdTomato (excitation at 554nm, emission at 581nm) (Shaner et al, 2004).

Table IV: The nucleotide sequence from Marchetti et al, 2000 of the nuclear localisation signal (NLS).

Localisation signal	Sequence
Nuclear localisation sequence (NLS)	CGAGGACACAAGCGGTCACGTGAA

To increase the fluorescent signal, it is recommended to concentrate the fluorescent protein inside of the nucleus. For that purpose, we employed experimentally verified 8 amino acids long nuclear localization sequence (NLS) (Table IV) that targets proteins of interest into the *T. brucei* nucleus (Marchetti et al., 2000). In summary, for the pilot experiments we generated 4 different constructs containing: i) mNeonGreen+NLS; ii) mNeonGreen-NLS; iii) tdTomato+NLS; iv) tdTomato-NLS.

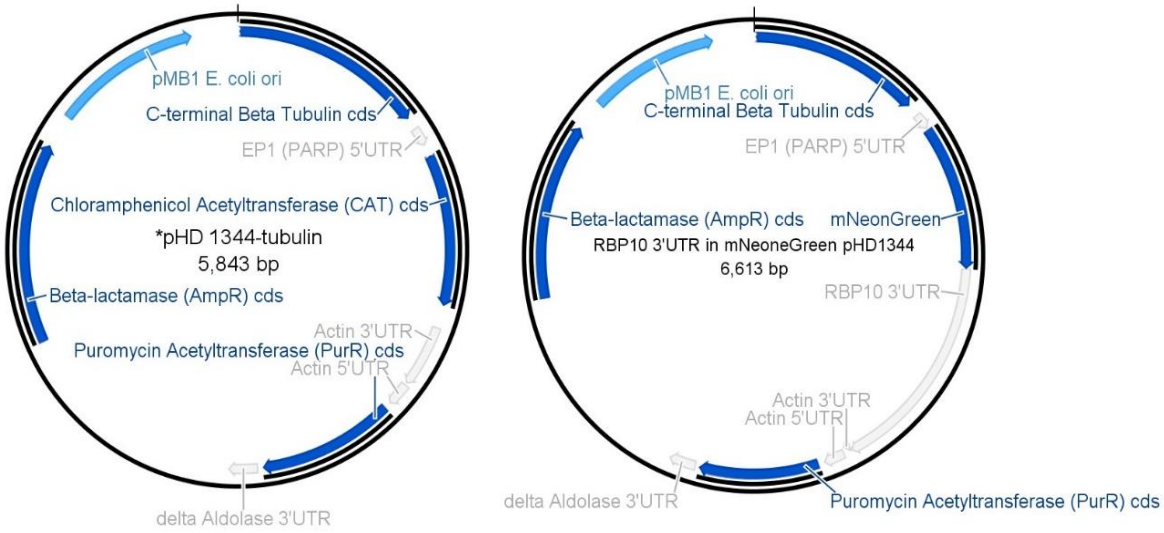

Figure 4: Plasmid map of pHD1344 created in Geneious software before modifications (left) and after modifications with RBP10 3'UTR insertion (right).

The constitutive expression of genes of interest was achieved by their stable integration to specific regions of the *T. brucei* genome. We used pHD1344 plasmid (Haile et al, 2003), which integrates genes of interest into the β-tubulin locus by homology recombination. The plasmid contains the β-lactamase gene that is responsible for the ampicillin resistance (AmpR) in bacterial cells, the *E. coli* replication origin pMB1 and the puromycin cassette (PurR) joint to actin 5'UTR, which is used as a selective marker for trypanosomes. The original pHD1344 plasmid also encodes the chloramphenicol acetyltransferase (CAT), a reporter gene which activity can be easily measured in order to test putative promoters and other regulatable regions (Gorman et al, 1982).

First, we replaced the CAT gene with genes for fluorescent proteins mNeonGreen or tdTomato. For that purpose, the plasmid was digested with HindIII and BamHI restriction enzymes (1 hour, 37°C), separated on DNA gel electrophoresis and extracted from gel.

Second, the inserts of interest representing mNeonGreen or tdTomato genes were generated similarly by cleaving them from pGEM-T easy plasmids using HindIII and BamHI restriction enzymes and purifying them from gel after the agarose electrophoresis. Then the inserts were ligated into the linearized pHD1344, ligation mixture was transformed into the bacterial cells, bacterial clones were confirmed by restriction digest and the final plasmids were verified by sequencing.

Finally, we created new unique restriction site between the 3′ end of the gene of interest and 5′ end of the actin 5′UTR (Figure 4) to facilitate the cloning of various 3′UTRs,

which will affect expression of the fluorescent proteins. The KpnI restriction site was created by mutagenesis using QuikChange Lightning Site Directed Mutagenesis kit (Agilent Technologies). The first step of mutagenesis was to design oligonucleotides which would serve as primers to generate a new plasmid. These oligonucleotides contain mismatches in the middle of their sequence, as it is the place, where mutation should occur to create the new restriction site. The rest of the primer sequence is unmodified in order to be complementary to the original plasmid and ensure efficient annealing during the PCR reaction. The primers were designed according to the instructions from the manufacturer and by using the web-based software available online at www.agilent.com/genomics/qcpd (Table V), synthesized and purified by liquid chromatography (HPLC) at Generi Biotech s.r.o.

Table V: Oligonucleotide sequence used for mutagenesis of the plasmid pHD1344 to create KpnI restriction site. KpnI restriction site is in italics, the mutated bases are marked in bold. Sequences are displayed in the direction 5' → 3'.

Orientation	Code name	Sequence
Fw	AZ0825	AACGCATCAAACACAACTG***GT****AC*CACTATTTCA ATCATGTCGAC
Rv	AZ0824	GTCGACATGATTGAAATAGT*GGT****AC****C*AGTTGTG TTTGATGCGTT

To generate the mutagenized plasmid, we employed PCR reaction. All the necessary components for the site directed mutagenesis of the plasmid in 25µl reaction are listed in Table VI. The cycle parameters are displayed in Table VII.

Table VI: The composition of mutagenesis mix.

Solution	Volume
10xreaction buffer	2.5µl
dsDNA template (22ng)	1µl
125ng of oligonucleotide 1 (Fw)	1µl
125ng of oligonucleotide 2 (Rv)	1µl
dNTP mix (each dNTP 10mM)	0.5µl
QuikSolution reagent	1.5µl
ddH2O	17µl
QuikChange Lightning Enzyme	1µl

Table VII: The PCR conditions for site directed mutagenesis.

Segment	Cycles	Temperature	Time
1	1	95°C	2 minutes
2	30	95°C	20 seconds
		68°C	10 seconds
		68°C	3 minutes
3	1	68°C	5 minutes

To ensure that only the newly amplified and thus mutagenized plasmids are transformed into the *E. coli* cells, the PCR mixture was digested with DpnI enzyme. This restriction enzyme recognizes methylated restriction site and therefore, only the template plasmid DNA is digested, while the new plasmids stay uncut. The digestion was performed by adding 1µl of DpnI into the PCR mixture and incubating it at 37°C for 5 minutes.

The last step of the site directed mutagenesis was transformation into the competent cells (XL1-blue). The transformation was performed according to the information provided in the manual. Purified plasmids were verified by restriction digest using KpnI and HindIII enzymes (1 hour, 37°C). Subsequently, correct plasmids were sent for sequencing.

Finally, the 3´UTRs of BARP_15610 and RBP10 were introduced into the plasmid via XhoI and KpnI restriction sites. Both plasmids were generated under the same

conditions. The 10µl ligation reaction contained insert DNA (3´UTR for either BARP_15610 or RBP10) and linearized vector (pHD1344) in ratio of 3:1, 1µl of T4 ligase (1U/µl) and 1µl of 10x ligase buffer. This reaction mix was incubated at 4°C overnight. The transformation was performed as described in previous chapter (3.3).

3.5. Generation of genetically modified *T. brucei* cells

As a parental cell line for the transfection of previously described constructs we used RBP6 overexpression cells.

The RBP6 overexpression cells in mid-log phase (0.6-1x10^7 cells per ml) were harvested (total cell number 5x10^7/transfection) by spinning them down at 1300g at 4°C for 10 minutes. The cell pellet was washed with 10ml of ice-cold phosphate saline buffer with glucose (PBS-G) (1300g, 4°C, 10 minutes). Linearized sterile DNA (10µg) was pipetted into gap cuvette provided in Amaxa™ Human T Cell Nucleofector™ Kit (Lonza). The cell pellet was resuspended in 100µl of AMAXA Human T-cell solution (81.8µl Human T-cell nucleofector solution + 18.2µl Supplement). Next, the resuspended cells were transferred into the electro-cuvette with DNA. The cuvette was then placed into AMAXA device (Nucleofector™ II, Lonza) where electroporation occurred (program X-014). Subsequently, the cells were transferred into a flask which already contained 6ml of SDM-79 media with 10% FBS and incubated at 27°C for 16-18 hours. Then 6ml of new media with 2x concentration of selective drug was added. The final concentration of puromycin was 1µg/ml. The cells were then serially diluted into 24-well plate to facilitate the cloning of transfectants.

3.6. Fluorescence-activated cell sorting (FACS) of fluorescent protein expressing cell lines

FACS is a specialized form of flow cytometry. The flow cytometry is an analytical technique for cell counting, sorting and biomarker detection as the cells go one by one in the trajectory of laser light which provides them with excitation energy that is transformed to emission light caught by detector in the flow cytometer (Figure 6). This information is analysed together with information about the size (forward scatter = FSC) and the complexity of granularity of the cells (side scatter = SSC) creating this way a complex information about each single cell. (http://www.facs.ethz.ch/education.html)

The single cell analysis is reached by a hydrodynamic focusing. The middle stream containing the cell suspension is pressured differently than the streams on the sites. The injection rate of the sample is controlled via this differential pressure mechanism (Ibrahim and Engh, 2007). Finally, the signals are then interpreted on a computer screen (Figure 6).

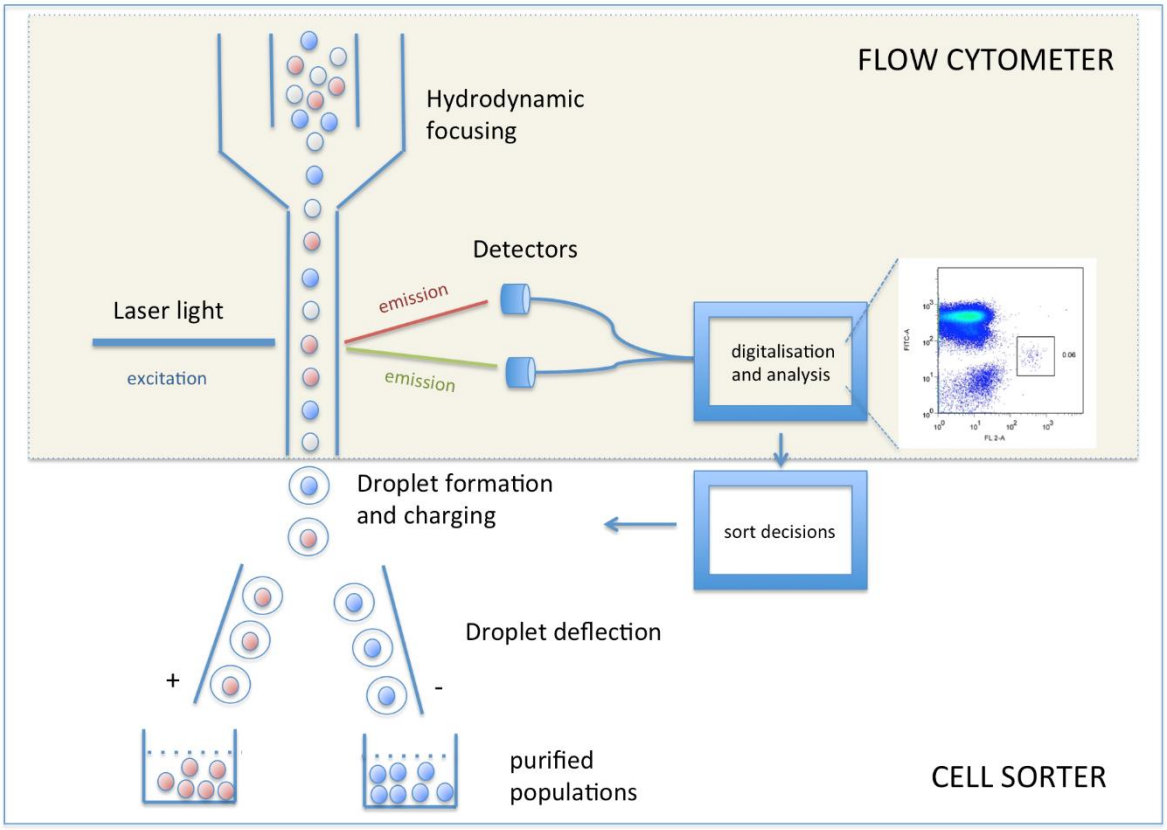

Figure 5: Schematic representation of flow cytometer and cell sorter analysis (http://www.facs.ethz.ch/education.html).

For our experiment we spun down $5x10^6$ cells for 10 minutes at room temperature (RT), washed them with 1ml of PBS pH 7.4 and spun again for 10 minutes at RT. The supernatant was discarded and the cell pellet was resuspended in 2ml PBS pH 7.4. The samples were then analysed in the BD FACS Canto II (BD Biosciences). The FITC filter was used to detect mNeonGreen fluorescence, while the PE filter was used to detect tdTomato fluorescence.

3.7. Detection of fluorescent signal by fluorescent microscopy

Another possibility, how to detect fluorescent protein and confirm specificity of the gene expression, is to employ fluorescent microscopy. In the same way as the FACS machine, a laser excites the fluorescent proteins expressed in the cells, and the emission signal is then detected under specific filter on fluorescent microscope.

First, the surface of the cover glass was covered by poly-L-lysine (Sigma-Aldrich®). This procedure is used to enhance cell attachment and adhesion to the glass surface. Poly-L-lysine surface treatment is really needed only for BF, but since we were using differentiating cells some of them being metacyclic forms with BF surface features, we used poly-L-lysine glass for every sample. Firstly, 20µl of 10x diluted poly-L-lysine (stock solution 0.1%) were added on the cover slip and dried out at 37°C for 1 hour. After that, $1x10^7$ cells were harvested by spinning down at 1300g for 10 minutes at 4°C. Next, the cells were washed in 1ml PBS-G and spun down again. Subsequently, the harvested cells were resuspended in 100µl 1xPBS pH 7.4 and fixed with 100µl of 7.4% formaldehyde in 1xPBS. Next, 40µl of the cell suspension were applied to the cover slip and incubated for 15 minutes at RT in dark conditions to avoid the excitation of fluorescent protein from normal light. Afterwards, the buffer was removed and the cover slips were washed 3x with 100µl 1xPBS. After the last removal of the washed buffer, the cover slips were mounted on a glass slide with ProLong Gold Antifade Mountant (Invitrogen). The solution contains DAPI (4',6-diamidino-2-phenylindole), which binds to rich A-T regions in DNA present in the nucleus and kinetoplast in trypanosomes.

Images were taken under different light conditions with the fluorescent microscope (Axioplan 2 imaging Universal microscope, Zeiss) with CCD camera (Olympus DP73). The FITC filter was used for mNeonGreen, while the PE filter was used to detect tdTomato. The nucleus and kinetoplast were visualized under the DAPI filter. The morphology of the cells was examined under polarized light.

3.8. Sorting of RBP6_mNeonGreen_RBP10 cell line using a cell sorter

Heterogeneous mixtures of cells can be physically divided via a cell sorter. It has all the features of the flow cytometer and in addition to that it is able to sort the cells according to their type. The components are in the first step (analysis of the cells) the same as in the FACS analysis (Figure 6). However, the cell sorter has additional characteristics. One of

the differences is the ability to create a droplet. Passing cells one by one are separated to small objects (droplets) by acoustic wave (Ibrahim and Engh, 2007). Next, the signal from the cells is analysed. In return, the droplet with a single cell obtains an electric charge. Then the cells are sorted in an electric field. Thus, cells with a negative charge will be drawn closer to the positive electrode and *vice versa*.

The cell samples were prepared as described previously (chapter 3. 6). In order to not clog the sorter, the cells were passed through a 50µm filter (CellTrics®, Sysmex) and sorted using the S3™ cell sorter (Biorad). Subsequently, the cells were collected into 5ml falcon tubes with 500µl of media (SDM-80). Sorted cells were spun down 1300g for 10 minutes at RT. The cell pellet was resuspended in the conditional media to better recover the cell growth. The final concentration of the cells was approximately $2x10^6$/ml. This culture was then incubated shaking 90rpm at 27°C for 2 hours and then, the viability was visually monitored under the light microscope.

3.9. Generation of TbIF1 double knock-out (dKO) cell line

Gene knock-out is an experimental technique by which the expression of a gene is fully eliminated. This approach uses the homologous recombination, a process naturally occurring in cells, to replace coding sequence (cds) of the gene by desired construct. The dKO strategy is performed in two steps. First allele of the gene gets knocked out usually by one selectable marker (e.g. neomycin), and when the single-knock out cell line (sKO) is established, the second allele is replaced by a different construct carrying another selectable marker (e.g. hygromycin).

Table VIII: Primers used for amplifying the 5' and 3' UTR regions of TbIF1 with shown added restriction sites. Underscored letters or letters in italic correspond with introduced restriction sites. Sequences are displayed in the 5'→3' direction.

Primer name	Code name	Introduced Restriction site	Sequence
5'UTR Fw	AZ0831	NotI	ATAGCGGCCGCCTATTAGTGATAACCAAGGGG
5'UTR Rv	AZ0832	MluI, *XhoI*	ATAACGCGT*CTCGAG*GGAACCTCTCCTTCACTTTATCC
3'UTR Fw	AZ0833	XbaI, *SwaI*	ATATCTAGA*ATTTAAAT*GAAGGAGCAGGCGTCATTC
3'UTR Rv	AZ0834	StuI, *NotI*	ATAAGGCCT*GCGGCCGC*TGCCCCAGTTGTGTCGG

To use homologous recombination to knock-out TbIF1 (T927.10.2970), cassettes containing the selectable markers were flanked by short sequences of TbIF1 5'UTR (542bp) and 3'UTR (412bp). To facilitate cloning, restriction sites NotI, MluI, XbaI, XhoI, StuI, SwaI were added to the designed primers (Table VIII). The PCR mixture was prepared as shown in Table II and the PCR conditions were the same as described in Table III with two modifications: the annealing temperature was set to 55°C, and the extension step was set to 30 seconds. PCR fragments were resolved on 1% agarose gel, cut out and gel extracted.

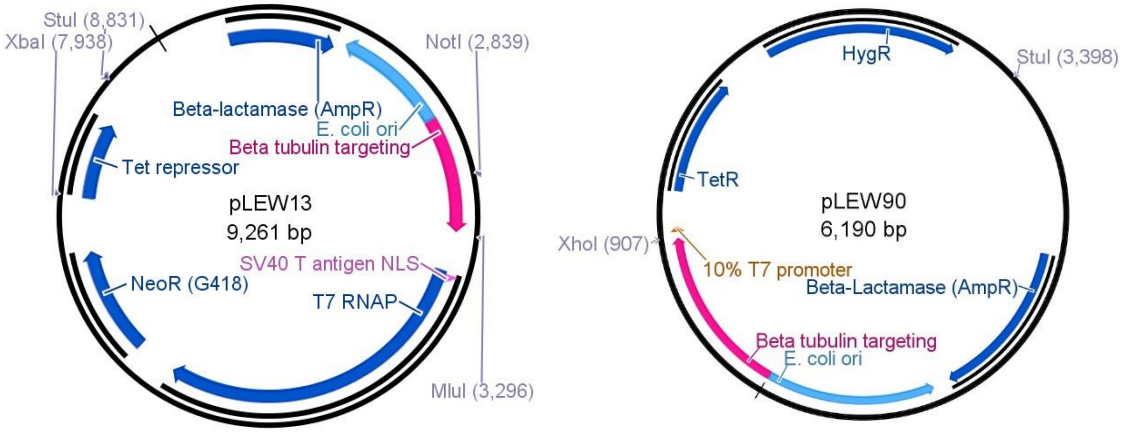

Figure 6: The plasmid map created in Geneious software of pLew13 (left) and pLew90 (right) with highlighted restriction sites used for subsequent cloning steps.

The TbIF1 5'UTR and 3'UTR fragments were cloned into pLew13 (Wirtz et al, 1999) vector using the appropriate restriction sites. The extracted PCR fragments were directly digested with NotI and MluI (5'UTR) or XbaI and StuI (3'UTR) (Figure 7) for 1 hour at 37°C, separated on 1% agarose gel and gel extracted. First, 5'UTR fragment was ligated to linearized pLew13 plasmid and after the verification of successful cloning, the 3'UTR fragment was ligated as well. Then, modified pLew13 plasmid was digested with NotI for 3 hours at 37°C, hence, cutting out a cassette containing the T7 RNAP and a resistance marker for Geneticin (NeoR/G418) flanked with 5' and 3' TbIF1 UTRs. Consequently, this cassette was transfected into the wt PF cells as described in chapter 3.5.

It is generally accepted that a gene replacement by homologous recombination is not very efficient process and the correct genome rearrangement will occur only in a few cells. The PF are very sensitive to the low cell density and for that reason, it is difficult to obtain knock-out cells after the transfection. In order to obtain a viable culture of KO PF cells,

wt PF cell were placed into each well at the concentration of $5x10^4$ cell/ml a day before the transfected cell were added to create the conditional media in the wells. Then the transfected cells were added together with the appropriate amount of the selective drug (G418 15µg/ml, for Hygromycin 25µg/ml) and the plates were incubated at 27°C for 3 weeks. Every other day dead cells were removed from the plates. After the selection process the obtained cell lines were screened for correct gene replacements by PCR.

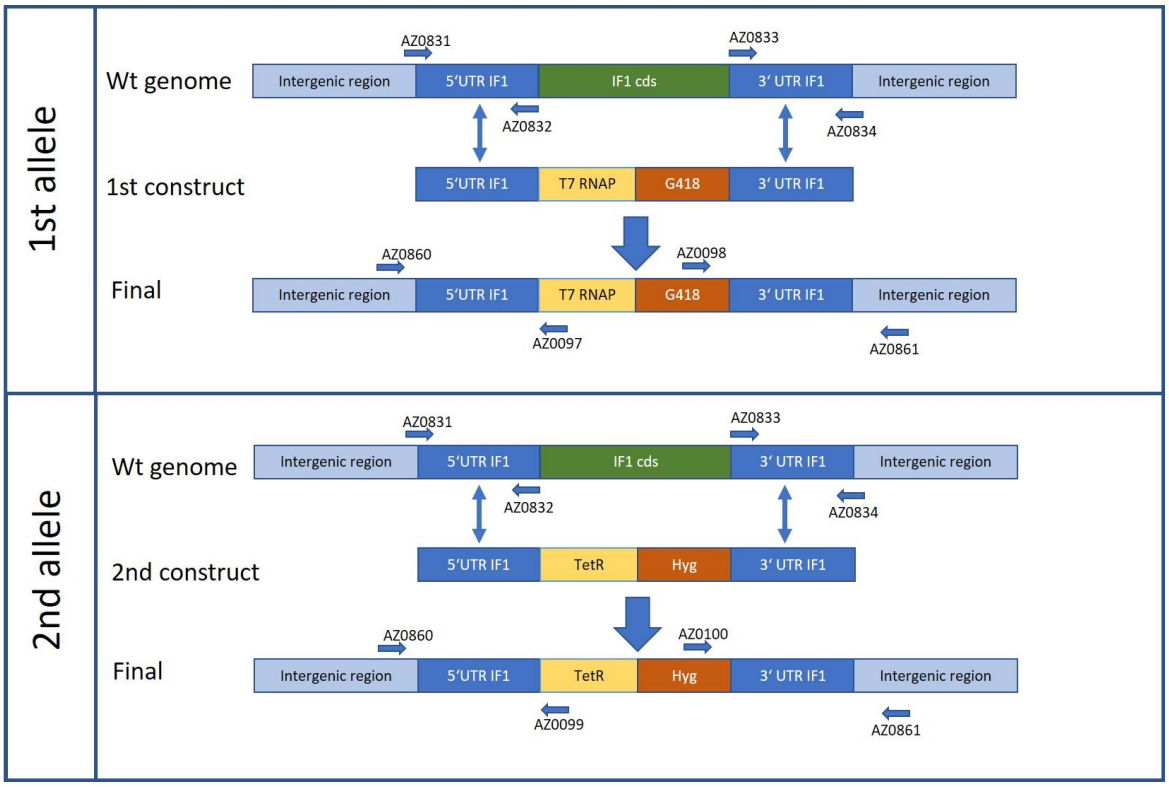

Figure 7: Scheme of TbIF1 dKO with annotated primers and their annealing positions. wt - wild type.

To knock-out the second allele, the pLew90 (Wirtz et al, 1999) vector was digested with XhoI and StuI for 1 hour at 37°C (Figure 7) to excise a cassette, which contains hygromycin resistance and tetracycline repressor. This cassette was used to replace the neomycin containing cassette in the modified pLew13 vector. Consequently, the cassette containing hygromycin resistance and tetracycline repressor flanked with 5' and 3'UTR regions from TbIF1 gene, was digested with NotI restriction enzyme for 3 hours at 37°C and transfected into the verified sKO cell line. The transfection was performed under the same conditions as described for the sKO. The selection for transfectants lasted 3 weeks as well.

Table IX: Summary of used primer pairs for the examination of inserted sequence in KO strategy with the specific annealing temperatures and extension times differing from previously shown PCR reaction (Table III).

Primers	PCR product	Annealing temperature	Extension time
AZ0097 **AZ0860**	1147bp	52°C	1 minute and 30 seconds
AZ0098 **AZ0861**	1596bp	52°C	1 minute and 30 seconds
AZ0099 **AZ0860**	1387bp	52°C	2 minutes
AZ0100 **AZ0861**	1297bp	52°C	2 minutes
AZ0746 **AZ0747**	348bp	56°C	30 seconds

To examine the correct incorporation of the first and second cassette into the *T. brucei* genome several primer pairs were created (Figure 8, Table IX). To test the absence of TbIF1 in the genome, one primer pair (AZ0746 and AZ0747) was designed to amplify the TbIF1 cds. The genomic DNA from the cultures was extracted using a kit (GenElute™ Mammalian Genomic DNA Miniprep Kit, Sigma-Aldrich®) and subsequent PCR analysis was performed. The amplified DNA fragments were separated on 1% agarose gel and the correctness of the generated cell lines was evaluated based on the size of the amplified fragments.

4. Results

4.1. Selection of the suitable 3'UTRs to be joint with genes for fluorescent proteins

Initially, when this project started, we chose the life stage specific proteins based on the knowledge from the published research. In these research papers, BARP (Urwyler et al, 2007) and RBP10 (Wurst et al, 2012) were described as regulated proteins, which expression is switched on in certain life cycle stages (i.e. epimastigotes and metacyclics). To select the most suitable 3´UTR of the 14 different BARP genes we examined the unpublished transcriptomic data, which were kindly provided by Christian Tschudi laboratory. In their transcriptomic analysis, the relative abundance of trypanosoma mRNA levels was monitored in different tsetse fly organs (i.e. midgut, proventriculus and salivary glands). Upon our analysis, we selected BARP_15610 based on significant increase in transcript levels present in the proventriculus and salivary glands as these two organs are vastly colonized by epimastigote life stage (Vickerman et al, 1988).

To further verify our selected 3'UTRs, we wanted to detect the upregulation in protein expression as well. Thus, we analysed our proteomic data, which were acquired in collaboration with Dr. Falk Butter at the Institute of Molecular Biology in Mainz. The whole cell lysates were prepared from RBP6 overexpression cell line at days 0, 2, 3, 4, 5, 6 and 8 upon the tetracycline treatment (10ug/ml). Samples were prepared in quadruplicates and studied by label-free quantitative mass spectrometry. Volcano plot analysis was carried out to see the most prominent changes in the cellular proteome during the differentiation from the procyclic to metacyclic cells *in vitro*. Results for individual proteins are then presented in the form of a bar graph showing the relative level of protein at certain time points at a log2 scale.

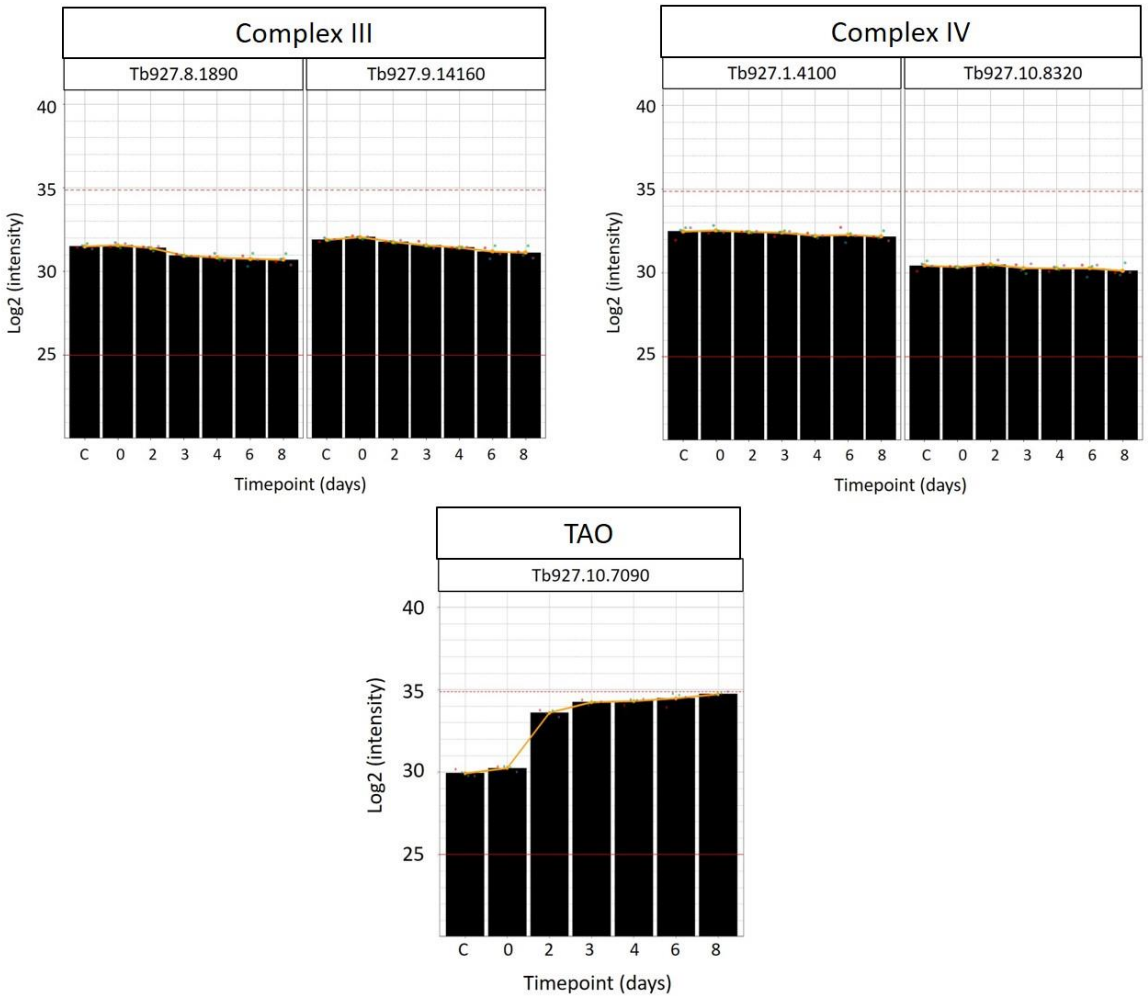

Figure 8: The change in relative protein expression during the differentiation in TAO and two subunits from complexes III and IV from ETC. C - control. The bars correspond with the median of LFQ (label-free quantification) intensities based on four independent measurements. The red dotted line represents the upper quantile (99% of LFQ intensities). The full red line represents lower quantile of measured LFQ intensities (1% of LFQ intensities). The orange line symbolizes the expression profile for each protein measurements created by bioinformatical approaches.

To assess the reliability of our proteomic data analysis, we decided to check the expression levels of the TAO (presumably to be up-regulated) and two subunits of respiratory complexes III and IV (presumably to be down-regulated). As expected the expression of TAO (Tb927.10.7090) was indeed upregulated at day 2, while two subunits of complex III, Tb927.9.14160 (rieske iron-sulfur protein) and Tb927.8.1890 (cytochrome c1) and two subunits of complex IV, Tb927.1.4100 (cytochrome oxidase subunit IV) and Tb927.10.8320 (cytochrome oxidase subunit IX) were down-regulated suggesting that the corresponding complexes are downregulated as well (Figure 9).

Then we used the proteomic data to assess the expression of BARP genes, which are specifically upregulated in epimastigote life cycle stage (Urwyler et al, 2007) and of RBP10 gene, which is specific for metacyclic life stage and bloodstream forms (Wurst et al, 2012).

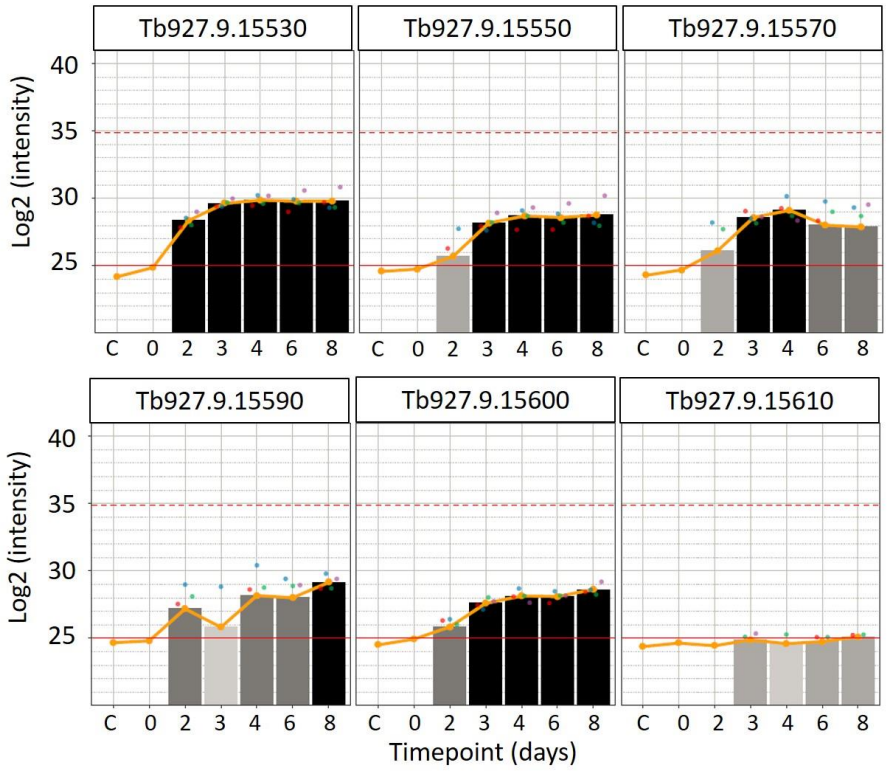

Figure 9: The change in relative protein expression of 6 BARP genes in differentiating cells. C- control. The bars correspond with the median of LFQ (label-free quantification) intensities based on four independent measurements. The red dotted line represents the upper quantile (99% of LFQ intensities). The full red line represents lower quantile of measured LFQ intensities (1% of LFQ intensities). The orange line symbolizes the expression profile for each protein measurements created by bioinformatical approaches.

According to the Tritryp database, *T. brucei* genome encodes for 14 proteins annotated BARP. However, only 6 were detected by our mass spectometry analysis (Figure 10). Nonetheless, a very distinct expression trend was shared by most detected BARP proteins. The proteins were not detected in control samples nor at day 0. A sudden steep increase of expression protein appeared around day 2 post tetracycline induction when culture contains epimastigotes. Based on these proteomic data, we suspected that the BARP_15610 will probably not be upregulated enough to create fluorescently labelled epimastigote stages as it has the lowest expression among the detected BARPs.

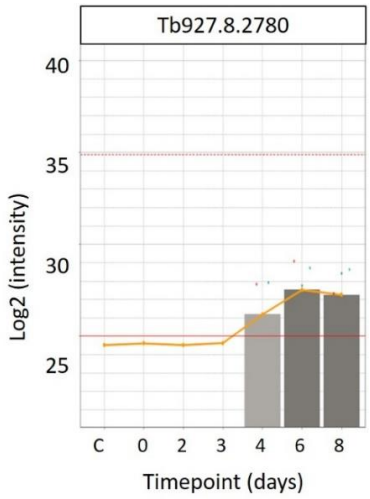

Figure 10: The change in RBP10's relative protein level during cell differentiation. C – control. The bars correspond with the median of LFQ (label-free quantification) intensities based on four independent measurements. The red dotted line represents the upper quantile (99% of LFQ intensities). The full red line represents lower quantile of measured LFQ intensities (1% of LFQ intensities). The orange line symbolizes the expression profile for each protein measurements created by bioinformatical approaches.

Very distinct expression pattern was also detected for RBP10 (Tb927.8.2780) (Figure 11). The protein was first detected at day 4 after the RBP6 induction, first day when the metacyclic trypanosomes were appearing in the culture. Our analysis suggests that 3'UTR of RBP10 might be suitable to regulated expression of fluorescent proteins.

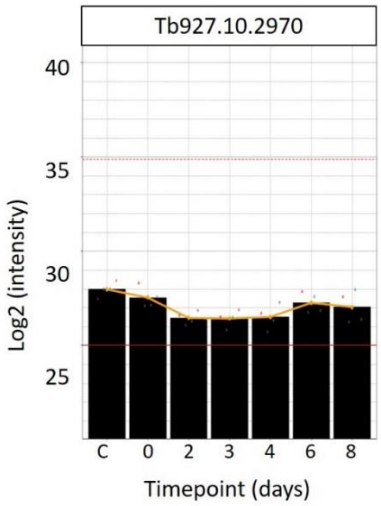

Figure 11: The changes in the protein level of TbIF1 in cells during differentiation. C – control. The bars correspond with the median of LFQ (label-free quantification) intensities based on four independent measurements. The red dotted line represents the upper quantile (99% of LFQ intensities). The full red line represents lower quantile of measured LFQ intensities (1% of LFQ intensities). The orange line symbolizes the expression profile for each protein measurements created by bioinformatical approaches.

Last, but not least, we checked the expression levels of TbIF1 (Tb927.10.2970), since in certain cancer cells the expression of its homologue, IF1, is increased during the metabolic rewiring from OXPHOS to aerobic glycolysis (reviewed in García-Bermúdez and Cuezva, 2016). In contrast to the published data from the mammalian system, the expression of TbIF1 was slightly decreased during the RBP6 over-expression. This protein was previously shown to be expressed only in PF, since its expression is lethal for BF cells. So, our mass spectrometry data are in agreement with its function of being the inhibitor of FoF1 ATPase (Pullman and Monroy, 1963; Panicucci et al, 2017) and its role during the procyclic stage differentiation must be experimentally examined.

4.2. Constitutive expression of fluorescent proteins in noninduced RBP6 overexpression cell line cells

The final goal of this project was to generate a cell line, in which expression of a fluorescent protein will be specifically regulated during the insect life stages differentiation and thus it would be possible to sort specific life cycle stages by cell sorting. For pilot experiments we first generated cell lines, which express fluorescent proteins constitutively These cell lines were named:

I. PF_mNeonGreen_Act

II. PF_NLS_mNeonGreen_Act

III. PF_tdTomato_Act

IV. PF_NLS_tdTomato_Act

Constitutive expression of the fluorescent protein was achieved by the presence of 3'UTR for actin. The cell lines I to IV were used for pilot experiments in which we tested if the fluorescence can be detected by FACS and fluorescent microscopy and if the localisation of the fluorescent proteins into to nucleus generates stronger signal.

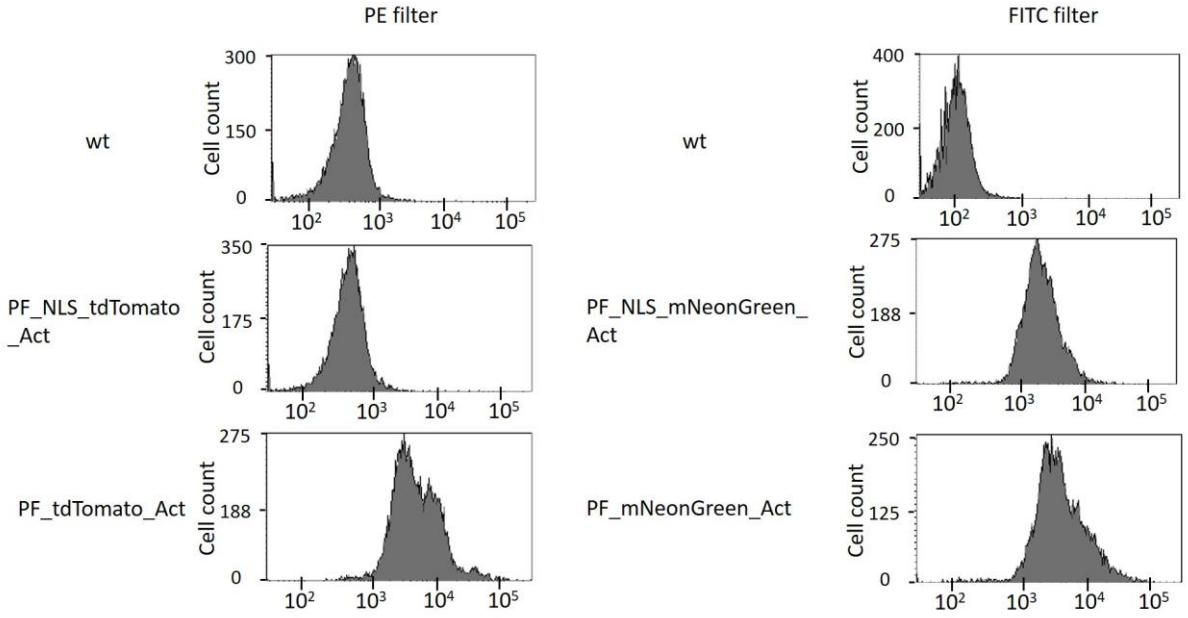

Figure 12: Histograms from FACS detecting fluorescence under two different filters with cell lines constitutively expressing one of two fluorescent proteins under the control of actin 3'UTR. Left: PE filter for tdTomato expressing cells; Right: FITC filter for mNeonGreen expressing cells. Wt - wild type.

Four different RBP6 overexpression cell lines which express mNeonGreen or tdTomato with or without NLS were analysed by the FACS machine. The fluorescence of tdTomato was detected with the PE filter, mNeonGreen fluorescence was detected with the FITC filter (Figure 13) and most importantly, a visible shift in the fluorescence intensity was observed in comparison to wt cells. Interestingly, the fluorescence signal was not stronger for cells in which the fluorescent protein was localized to nucleus (PF_NLS_tdTomato_Act, PF_NLS_mNeonGreen_Act) (Figure 13).

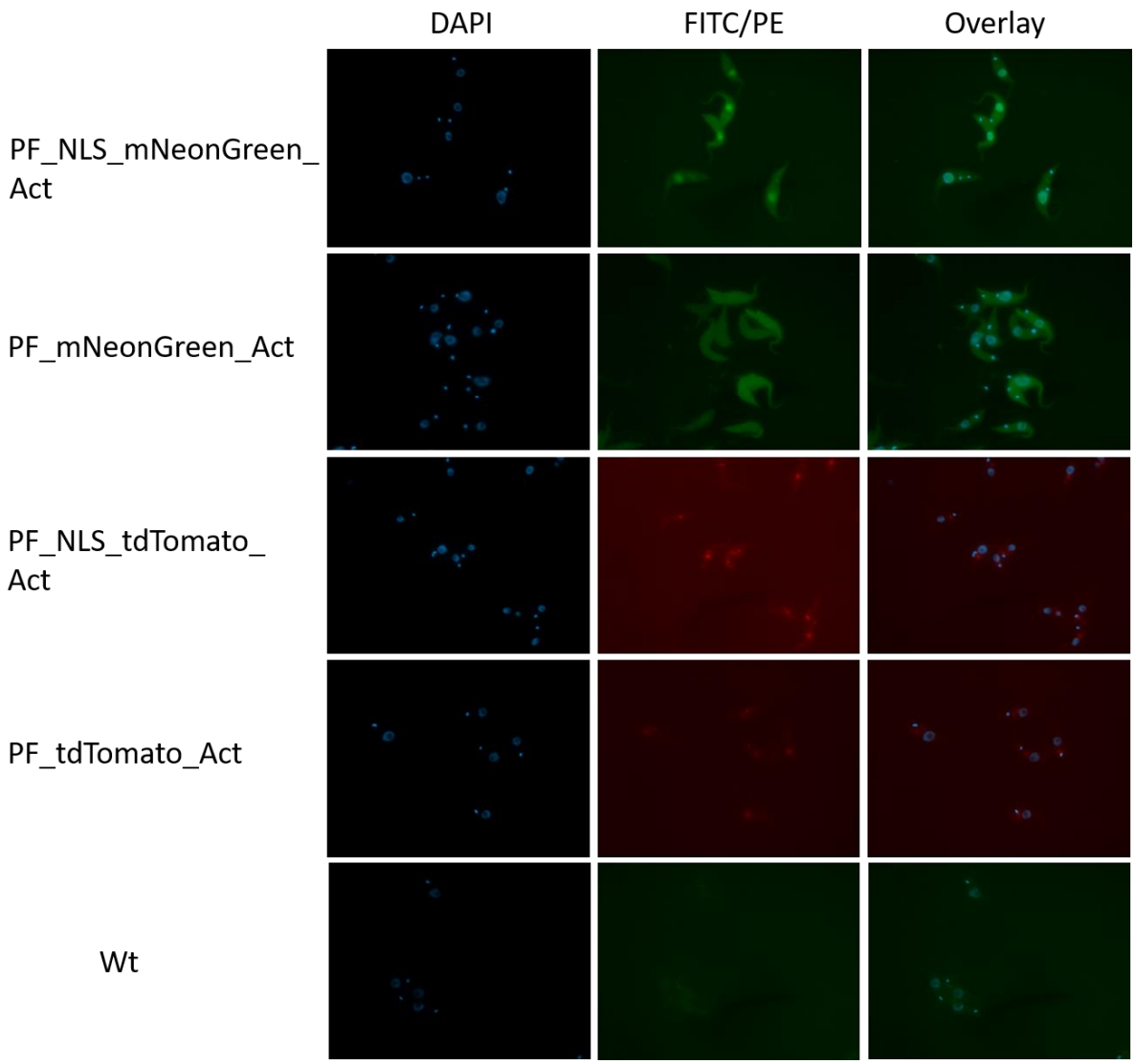

Figure 13: Cell lines constitutively expressing one of two fluorescent proteins (mNeonGreen or tdTomato) under control of actin 3'UTR. FITC filter for mNeonGreen cell lines, PE filter for tdTomato cell lines. Wt - wild type.

To check if the fluorescent proteins were indeed targeted to the nucleus we examined the cell lines under the fluorescence microscope. The presence of NLS in the sequence of mNeonGreen was sufficient to target this protein to nucleus. Nevertheless, in agreement with the FACS data, the fluorescence was not better visible compared to PF_mNeonGreen_Act cell line (Figure 14). Unfortunately, the tdTomato did not produce a good fluorescent signal in either cell line (PF_tdTomato_Act or PF_NLS_tdTomato_Act). The reason for the lack of signal is that tdTomato fluorescence is sensitive to fixing solution and can be detected only in live cells. Thus, this protein will not be suitable for our future experiments and we decided not to use tdTomato for further studies. We continued only with PF_mNeonGreen_Act and replaced the 3'UTR for actin with either 3'UTR of BARP_15610 or 3'UTR of RBP10.

By this replacement RBP6_mNeonGreen_RBP10 and RBP6_mNeonGreen_BARP_15610 cell lines were created.

4.3. Regulated expression of mNeonGreen protein in RBP6 overexpressing cell line

The cell lines RBP6_mNeonGreen_RBP10 and RBP6_mNeonGreen_BARP_15610 were grown in SDM-79 medium and induced by tetracycline (2μg/ml) to trigger the differentiation. The RBP6_mNeonGreen_BARP_15610 was assayed at day 4 upon the tetracycline induction as the epimastigote forms are present at the highest concentration (Kolev et al, 2012). The RBP6_mNeonGreen_RBP10 was examined at day 10 post induction. Metacyclics are present in the culture at the higher concentration at this day (Kolev et al, 2012).

The fluorescence signal differed significantly between the two examined cell lines as the mNeonGreen_BARP_15610 fluorescence was very low, while the mNeonGreen_RBP10 fluorescence was well detected in non-induced and induced cell samples (Figure 15 and Figure 16).

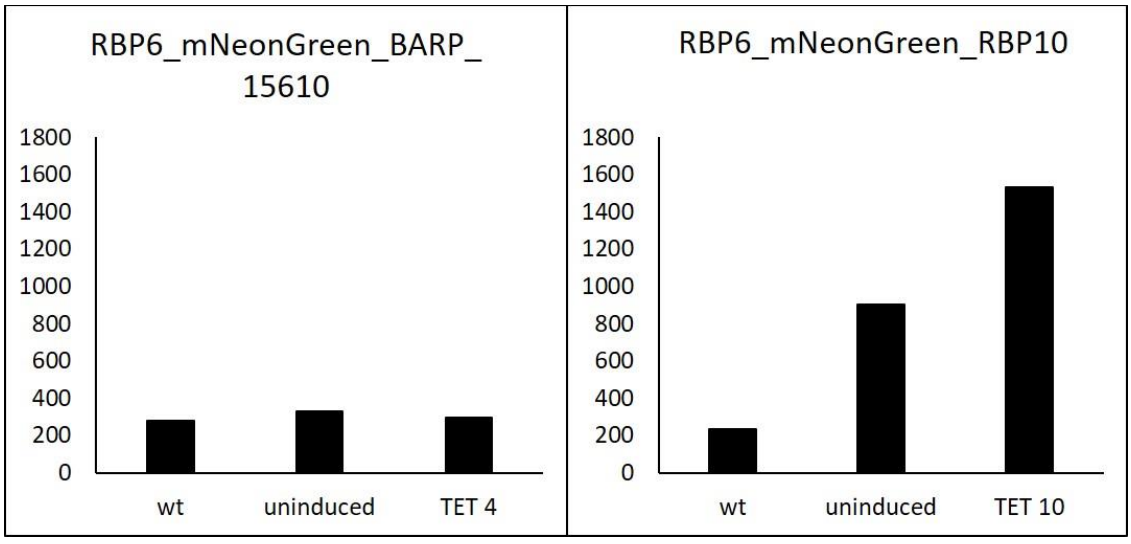

Figure 14: Fluorescence of differentiating cells with RBP6_mNeonGreen_BARP_15610 3'UTR (left) or RBP6_mNeonGreen_RBP10 3'UTR (right). TET 4 – 4 days after the initial tetracycline induction, TET 10 – 10 days after tetracycline induction, wt – wild type.

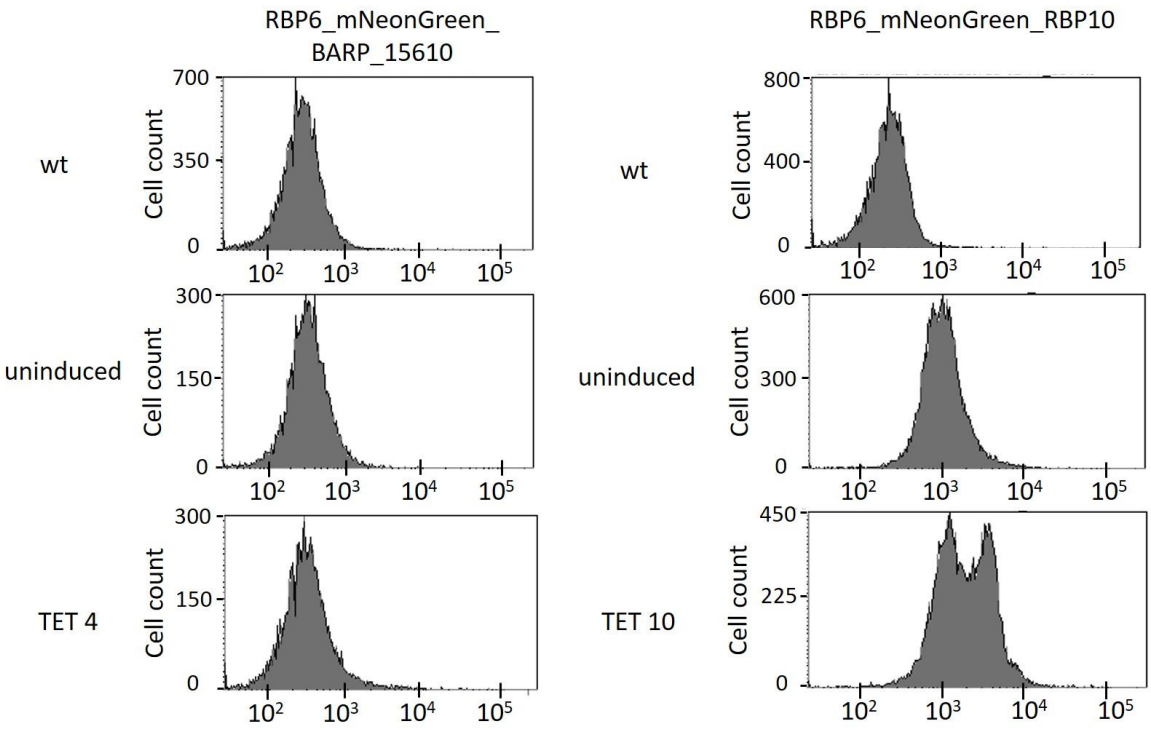

Figure 15: Different fluorescence in cell lines with mNeonGreen expressed under the control of BARP_15610 3'UTR (left) and RBP10 3'UTR (right) with comparison to wt (upper row). TET 4- 4 days since the start of tetracycline induction, TET 10 – 10 days since the start of tetracycline induction, wt – wild type.

Importantly, the fluorescence detected in RBP6_mNeonGreen_BARP_15610 did not increase during the induced differentiation suggesting that the 3'UTR region of the selected BARP_15610 gene did not cause the expected upregulation of mNeonGreen expression in epimastigotes (Figure 15, Figure 16). On the other hand, significant increase in the mNeonGreen fluorescence was observed in RBP6_ mNeonGreen_RBP10 induced sample (TET 10) compared to wild type and non-induced. Second fluorescent peak is readily detected at day 10 post tetracycline induction and might represent the differentiating cell population, i.e. metacyclic trypanosomes.

Similar results were obtained when fluorescence microscopy was used to examine the cell lines expressing mNeonGreen (RBP6_mNeonGreen_BARP_15610, RBP6_mNeonGreen_RBP10) in differentiating cells.

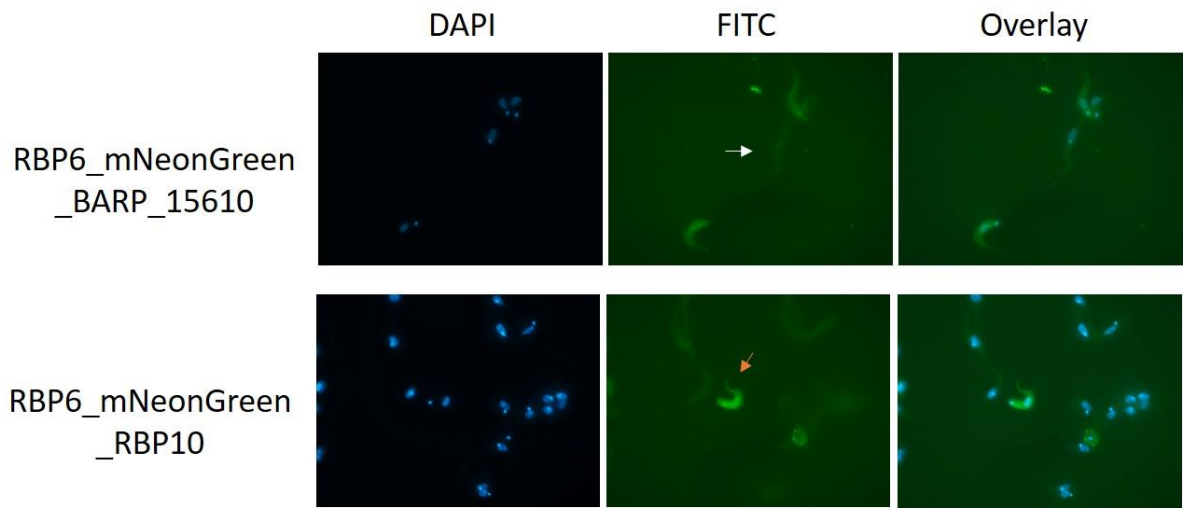

Figure 16: Detection of fluorescently shining cells under FITC filter detected by fluorescent microscope. White arrow – epimastigote stage, orange arrow – metacyclic stage.

Unfortunately, the tetracycline induced RBP6_mNeonGreen_BARP_15610 did not exhibit strong enough signal to be detected under the FITC filter (Figure 17). A barely visible cell is marked by a white arrow. This cell has a distinctly positioned kinetoplast in relation to the nucleus, which is a characteristic feature of epimastigote life stage. Typical procyclic-like cells which are found on the same image show even stronger fluorescence. Based on our analysis, we had to concluded that the chosen 3'UTR of BARP_15610 did not affect expression of mNeonGreen protein during the RBP6 induction and most likely different 3'UTR will have to be tested in order to specifically label epimastigote life cycle stage.

On the other hand, the RBP6_mNeonGreen_RBP10 cell line showed increased in fluorescence during the RBP6 induction (Figure 17). A clear difference in fluorescence is seen between the non-induced and tetracycline induced cells. A cell showing morphological signs of metacyclics (e.g. kinetoplast at the very posterior end of the cell) is expressing the fluorescent protein. Combining results from FACS and fluorescent microscopy we decided to use this cell line for a subsequent experiment with the S3 sorter.

4.4. Sorting of RBP6_mNeonGreen_RBP10 cells by S3 cell sorter

To sort the cell based on the fluorescence expressed in metacyclic life stage, the RBP6_mNeonGree_RBP10 cell line was used. In this experiment the cells were grown in

SDM-80 media – without glucose – and were induced with 5x more tetracycline (10µg/ml) than in the previous analyses. Lack of glucose and higher concentration of tetracycline in the culture resulted in more prompt differentiation (our unpublished observation).

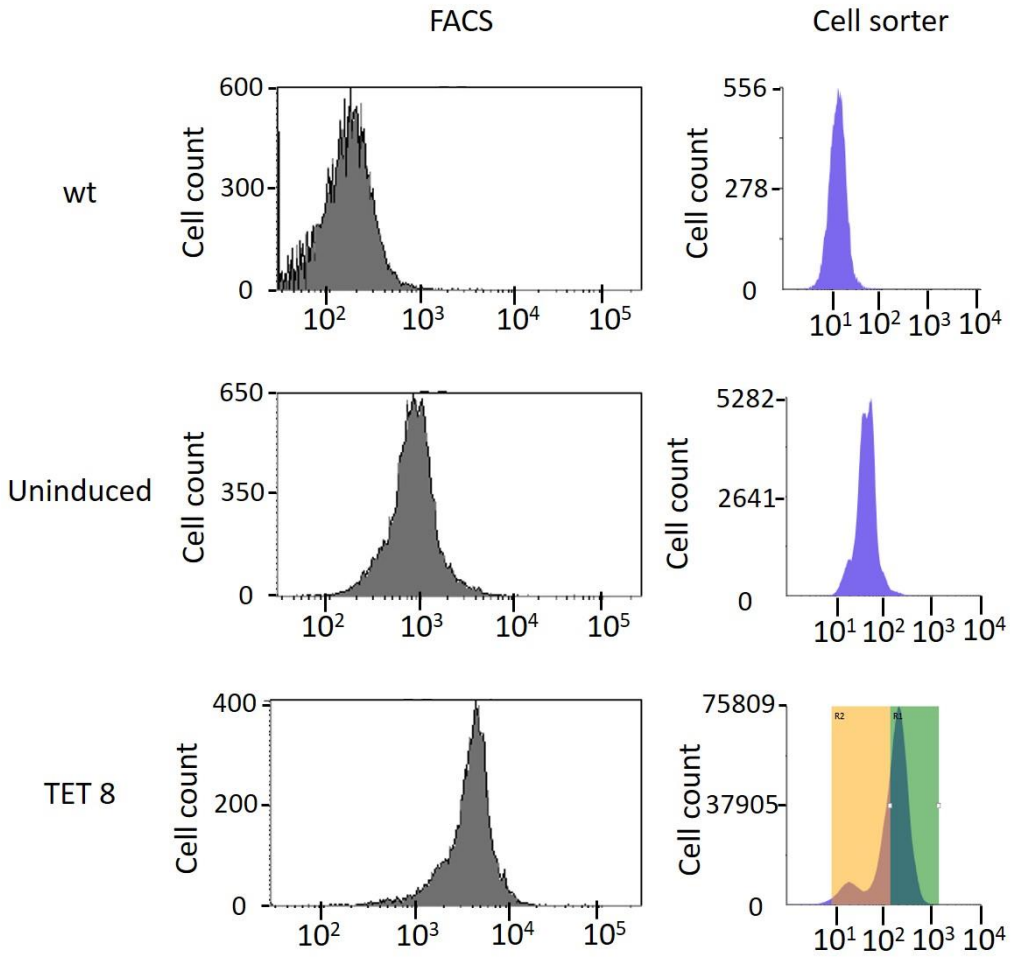

Figure 17 : Comparison of the detected fluorescence under FITC filter between FACS and cell sorter in the RBP6_mNeonGreen_RBP10 cell line. TET 8 – 8 days since the start of tetracycline induction, wt – wild type. Green box and peach box represent sorting gate.

First, the cell samples representing uninduced and cells induced for 8 days were analysed by the FACS machine to confirm the increase of fluorescence in the induced sample. Then the cell samples were also analysed by S3 cell sorter. The relative shift in fluorescence between uninduced and induced samples was compared (Figure 18). Both instruments were able to detect a shift in fluorescence between the uninduced and induced cells. The more fluorescent green area was gated as it should be enriched for metacyclic

cells. The less fluorescent peach area was sorted to different falcon tubes to obtain a culture of non-metacyclic cells (i.e. procyclic and epimastigote forms).

The viability of the cells was monitored after 2 hours in conditioned media. The cells were alive, quickly moving with expected morphology. This preliminary analysis suggests that the applied sorting process is able to produce enriched population of viable cells suitable for downstream analyses.

4.5. TbIF1 double knock-out (dKO)

TbIF1 was shown to trigger cellular responses as the switch from OXPHOS to glycolysis in cancer cells (reviewed in García-Bermúdez and Cuezva, 2016). Based on the similarities between the behaviour of cancer cells and *T. brucei* system, we were interested in exploring the hypothesis if *T. brucei* cells would be able to proceed with the differentiation, when TbIF1 gene is absent.

The single knock-out cell line was selected 3 weeks after the transfection. Several different cell lines were harvested for genomic DNA extraction and the integration of the sKO cassette was tested using PCR. The primers for verification were designed as shown in Figure 8 and the expected sizes of PCR products are shown in Table IX.

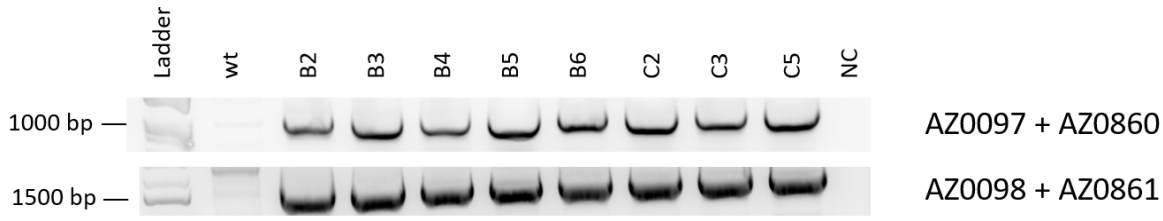

Figure 18: PCR test of the insertion of first construct for sKO by two different primer sets. AZ0097+AZ0860 were used for 5'end and AZ0098+AZ0861 for 3' end of the integration site. Wt – wild type, NC – negative control.

All selected cell lines showed PCR products of expected sizes with primer pairs for both 5' and 3' integration sites suggesting correct replacement of the first TbIF1 allele (Figure 19). Genomic DNA purified from wild type cells was used as a negative control and indeed no PCR products were detected in this reaction. Also, a control without DNA was run to ensure that primers were not contaminated with DNA. Clone C5 was chosen to be transfected with the dKO cassette to produce double knock-out cell line.

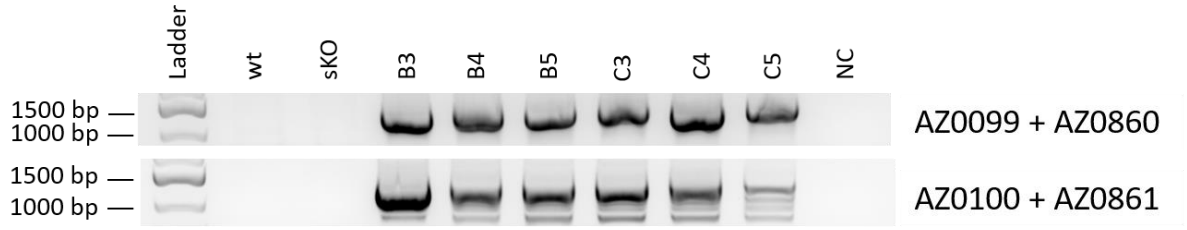

Figure 19: PCR test of the insertion of second cassette for dKO by two different primer sets. AZ0099 + AZ0860 were used for the 5' end and AZ0100 + AZ0861 for the 3'end of integration site. Wt – wild type, NC - negative control.

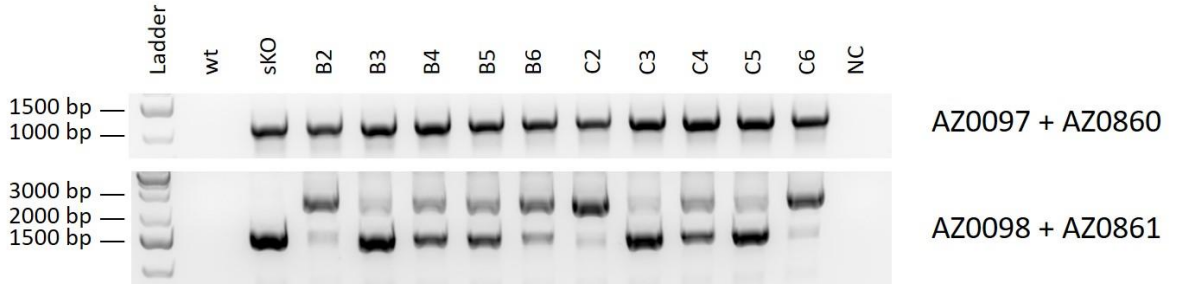

Figure 20: PCR test of the dKO for the first cassette by two different primer sets. AZ0097 + AZ0860 were used for the 5' end and AZ0098 + AZ0861 were used for 3' end of the integration site. Wt – wild type, NC - negative control. Clones B2, B6, C2, C6 were tested only for the first cassette as they were harvested latter and produced non-null mutant fragments by this analysis.

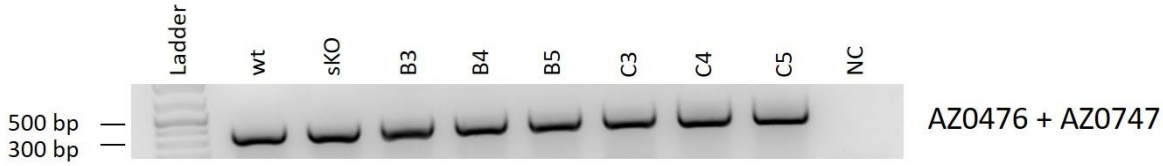

Figure 21: PCR test of dKO for the presence of TbIF1 cds with primer pair AZ0746 + AZ0747. Wt – wild type, NC - negative control.

The second transfection took 3 weeks as well and viable cell lines were tested for the proper integration of the second replacement construct. The verification primers were designed similarly as for the sKO and their positions are labelled in Figure 8. The PCR reaction gave very promising results, at the 3' and 5' integration sites for dKO cassette were amplified only in the selected dKO cell lines, and not in wt and sKO cell line (Figure 21). However, a control to confirm lack of TbIF1 ORF (open reading frame) showed a clear band for TbIF1 cds (Figure 22). Thus the 5' and 3' sKO integration sites were checked again. Unfortunately, we detected new PCR pattern (Figure 21), which suggests that during

the dKO selection a genomic arrangement took place and dKO cell lines are not true null mutants.

5. Discussion

5.1. Analysis of proteomic data

The RBP6 induced cell line was analysed by label free quantitative mass spectrometry in collaboration with Dr. Falk Butter, Institute of Molecular Biology, Mainz. After it was possible to access the proteomic data showing the relative protein expression during the *in vitro* induced PF differentiation, the results were validated by comparing the obtained data with previous findings about mitochondrial regulation during the *T. brucei* life cycle. For example, the dimeric final plant-like oxidase TAO is more abundant in BF as this enzyme is used for respiration (Smith et al, 2017). In our data set, the relative protein levels of TAO were increased as the differentiation was progressing. Respiratory chain complexes III and IV that pump protons across the membrane to create mitochondrial membrane potential in PF, are strongly downregulated in BF (reviewed in Lodish et al, 2000). Subunits from these complexes showed in our proteomic analysis continual decrease in relative protein levels as the differentiation was progressing. By using more examples (data not shown) we are confident that our proteomic analysis is in agreement with the previous knowledge.

Furthermore, the pattern of relative protein expression of six different BARP genes was shown to be consistent with the epimastigote forms appearance in the culture. The additional eight BARP proteins were not identified by our proteomic analysis and therefore the relative expression pattern could not be examined. The expression of BARP_15610 was shown to appear at day 3 upon induction and stayed at the same level until day 8 never reaching over the values for lower quantile of measured LFQ intensities. Importantly, this gene's 3'UTR was chosen to be joined with the fluorescent protein and transfected into *T. brucei* prior the proteomic data were available. At that time, we were able to confirm the expression of this protein only by available transcriptomic analyses (unpublished data, Kolev et al.) and the expression of BARP_15610 followed the expected pattern for epimastigote cells. Thus, the BARP_15610 3´UTR was selected as a suitable candidate for an epimastigote specific marker. However, our proteomic data showed, that most likely expression of fluorescent marker together with BARP_15610 3'UTR is not

strong enough to specifically label epimastigote life stages. Hence, it is important to analyse other BARPs 3'UTRs especially those whose expression is detected at day 2 upon the induction and reaches higher levels of relative protein expression. This is important to monitor as we expect that there is a threshold of protein level expression, which needs to be reached for detectable separation of the labelled cells using our sorting system.

Next, the proteomic data were used to verify RBP10 as a metacyclic marker. The upregulation of the protein was in agreement with literature where RBP10 was depicted as a BF specific protein (Wurst et al, 2012). Thus, RBP10 3'UTR was employed in our system. RBP6_mNeonGreen_RBP10 cell line was established and fluorescently labelled metacyclic cells were successfully detectable by fluorescent microscopy, FACS and cell sorter.

The inhibition of FoF1 ATPase by IF1 in cancer cell results in metabolic switches. It is also known that this protein can trigger ROS signalling in mammalian cells resulting in pro-survival and proliferative response (García-Bermúdez and Cuezva, 2016). Similar behaviour of cancer cells and our system led us to investigate the function of IF1 homologue TbIF1. Since IF1 inhibits FoF1 ATPase when this enzyme reverses its function in order to protect the cells in ischemic conditions (Campanella et al, 2008), it was not surprising that the expression of TbIF1 at the protein level was detected only in PF and not in BF (Panicucci et al, 2017). Thus, we were expecting to detect a downregulation of this protein during the differentiation from PF to metacyclics. However, the abundance of the protein was only slightly decreased during the *in vitro* differentiation. Therefore, our data suggest, that TbIF1 protein expression is being switched off later, most likely during the transition of metacyclic to BF in the bloodstream of the mammalian host.

5.2. Performance of fluorescent proteins during FACS and fluorescence microscopy

In order to sort epimastigotes and metacyclic trypanosomes we chose a method of an exogenic expression of fluorescent proteins in *T. brucei* and subsequent detection of these proteins by FACS and cell sorter. As a proof of concept, we generated four different cell lines (i.e. PF_mNeonGreen_Act, PF_NLS_mNeonGreen_Act, PF_tdTomato_Act and PF_NLS_tdTomato_Act), which expressed fluorescent proteins constitutively. The fluorescence was detected by FACS and under the fluorescent microscope. We expected

an increase in fluorescence when NLS was adjoined to the fluorescent protein in cell lines PF_NLS_mNeonGreen_Act, PF_NLS_tdTomato_Act, in which the fluorescent protein was targeted to nucleus. Nonetheless, such shift in fluorescence intensity was not detected in either mNeonGreen or tdTomato expressing cell lines. Fluorescent microscopy confirmed that mNeonGreen was indeed localized into the nucleus when the NLS signal was present (PF_NLS_mNeonGreen_Act). However, the fluorescence was also detected in the rest of the cell, presumably because of the high protein expression regulated by actin 3'UTR. In the cell line PF_mNeonGreen_Act the fluorescence signal was equally distributed throughout the whole cell as the NLS was absent.

Red fluorescent protein tdTomato proved not to be suitable for our experiments. In spite of the advertised photostability and brightness of this fluorescent protein (Shaner et al, 2005), we were unable to detect as strong fluorescence signal by either of used method. While a slight increase of fluorescence was detectable by the FACS analysis compared to wt cells, no fluorescence was detected by fluorescent microscopy. We suspected that the fixation step could have interfered with the function or stability of the tdTomato. However, there is no evidence of decreased stability or brightness upon fixing cells in the literature (Morris et al, 2010). When the live cells expressing tdTomato were monitored under the fluorescent microscope, the fluorescence was detectable. Nevertheless, no images were taken as the cells were moving too fast. We assume that this difference in stability and sensitivity of the red fluorescence protein to the fixation is simply a feature of these proteins, which are generally less photostable than green fluorescent proteins.

On the contrary to tdTomato, mNeonGreen was completely compatible with our analyses. It was stable enough to be monitored and visualized under the fluorescent microscope. The signal was also detectable on the FACS machine and the cell sorter. Thus, for the subsequent cloning was chosen mNeonGreen without the NLS and our molecular cloning resulted in generation of two additional cell lines: RBP6_mNeonGreen_BARP_15610 and RBP6_mNeonGreen_RBP10.

5.3. BARP_ 15610 3'UTR with mNeonGreen as a epimastigote specific marker

In the literature, BARP were successfully used to identify epimastigote life stage by anti-BARP antibodies (Rotureau et al, 2012; Urwyler et al, 2007). By proteomic analysis it was confirmed that the selected Tb927.9.15610 was expressed during the differentiation and

its expression patter was similar to the appearance of epimastigote life stages in the culture. Unfortunately, neither the FACS nor the fluorescent microscopy approaches were able to detect an increase in fluorescence after the RBP6 induction. There was only a slight shift in the relative fluorescence between the wt and noninduced cells, most likely due to a leaky expression of the system. Consequently, the fluorescence was tested at several different days to rule out any other life stage specificity. First detection was attempted 3 days post tetracycline induction. Subsequently, the analysis was carried out on days 4, 5, 7 and 10 after the start of tetracycline induction. Nonetheless, no shift in fluorescent signal intensity was detected (data not shown). These results are in agreement with our predictions based on the data from the proteomic analysis. The relative level of protein expression of BARP_15610 was not sufficient to secure strong protein expression specific for epimastigote life stage.

As the next step, different BARP 3'UTR will be used to drive the mNeonGreen expression in epimastigote life stage. The 3'UTR of BARP Tb927.9.15530 was already selected as another candidate, because of its highest expression among the detected BARP proteins in our proteomics analysis. This experiment should result in generation of RBP6_mNeonGreen_BARP_15530 and potentially mNeonGreen labelled epimastigote life stage upon RBP6 expression.

5.4. RBP10 3'UTR with mNeonGreen as a metacyclic specific marker

RBP10 is a BF form specific protein (Wurst et al, 2012), and our proteomic analysis confirmed this protein's life stage specific expression. Moreover, the mNeonGreen expression under the RBP10 3'UTR was detected first when the metacyclic cells were formed in the culture. Metacyclic cells expressed the fluorescent protein at high levels and these cells were easily detectable the under the fluorescent microscope compared to other life stages. Results from the FACS machine and the cell sorter represented by histograms (Figure 18) showed a shift in the relative fluorescence when metacyclic cells were present in the culture. This cell line experienced some low leaky expression of the fluorescent protein as well, as the uninduced cells exhibited higher fluorescence than wt. The culture after 10 days post tetracycline induction shows two distinct peaks on the histogram (Figure 16). The peak with higher fluorescence might represent metacyclic population, whereas the lower fluorescence peak may contain cells of other life stages.

Prior the sorting experiments, modification and adaptation of the protocol regarding the sorting speed, sorting media, recovery media and time for recovery were necessary in order to optimize the procedure. In the end, the cells were successfully sorted based on the different level of fluorescence. Immediately after the sorting, the viability of the cells was confirmed by light microscopy. Taken together, these results indicate the possibility to utilize our developed sorting approach for further analyses of live cells.

In the near future, we would like to continue with sorting of the induced RBP6_mNeonGreen_RBP10 cell line and verify the identity of the sorted metacyclics by uptake of fluorescently labelled dextran. The dextran assay has been already established in our lab and provides a nice tool to distinguish between PF and BF. Since only BF have enhanced endocytosis, the dextran molecules are up-taken by these cells in contrast to inactive PF. Figure 23 represents experimental data showing staining of PF and BF with 5mg/ml dextran. The Texas red filter was used for the visualization of dextran Alexa Fluor™ 568.

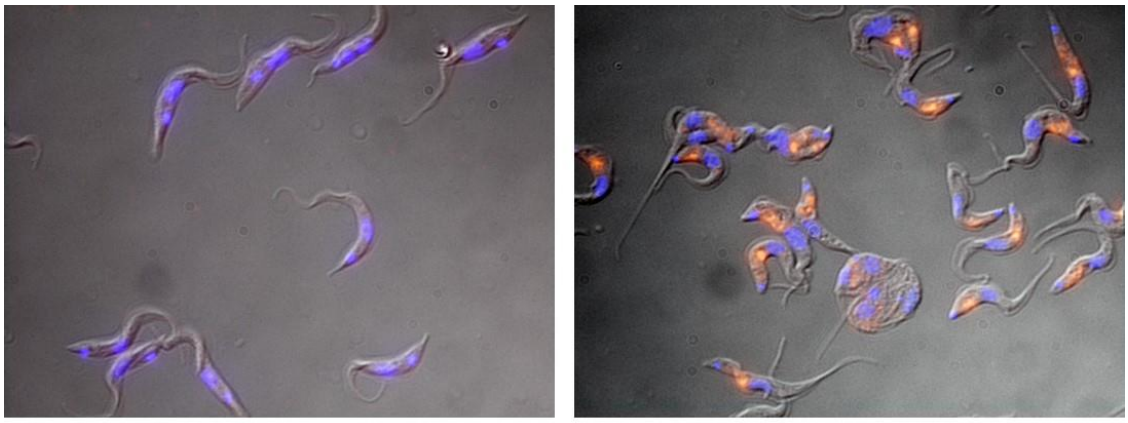

Figure 22: Dextran analysis with PF and BF cells visualized under the fluorescent microscope. Texas Red - a filter for dextran.

After establishing the RBP6_mNeonGreen_BARP_15530 cell line followed by successful sorting, several biochemical analyses on sorted epimastigote and metacyclic cell will be performed. For instance, the ATP production in different life stage will be monitored since different life stages can use different substrates (e.g. succinate, glycerol-3-phosphate, ketoglutarate) to produce ATP. Next, the mitochondrial membrane potential will be measured by safranin O assay with different inhibitors to assess which proton pumping

complexes contribute to the membrane potential. This is interesting to examine, since PF cells maintain the membrane potential by complexes I, III and IV, while BF cells generate the membrane potential by FoF1 ATPase (reviewed in Bringaud et al, 2006). When the mitochondrion becomes fully ATP-consuming organelle is not known. Furthermore, SDS-PAGE, western blots and native blots could be used to monitor the abundance of ETC complexes during the differentiation. We expect to reveal downregulation of complexes I, III and IV. Moreover, the changes in mitochondrial morphology happening during the *in vitro* differentiation can be studied by cryotomography. We expect to detect less cristae in the metacyclic cells resembling the BF, which have a tubular mitochondrion without branches. For this analysis, it will be very important to have a pure culture of only one life cycle stage as only mitochondria are examined and thus morphological marks used for identification of the certain life stages are not visible.

5.5. TbIF1 dKO

Since it was previously shown that IF1 is capable of triggering ROS production, which results in cellular responses in cancer cells during the reprogramming from OXPHOS to aerobic glycolysis (Formentini et al, 2012), and since there is a possible analogy between the cancer cells and our system, we wanted to explore the involvement of TbIF1 in the signalling during the *T. brucei in vitro* differentiation.

While the generation of the TbIF1 sKO was without major difficulties, the generation of dKO was not successful. The cell lines, which were selected after the transfection of the dKO cassette were screened for proper integration of this cassette into the *T. brucei* genome. Promising results were detected since the PCR fragment size suggested correct replacement of the TbIF1 cds in the second allele. However, subsequent PCR analysis designed to detect no TbIF1 cds failed and a band of the predicted size was detected. This result suggests that TbIF1 ORF is still present in the genome of *T. brucei* and the selected cell lines are not true double knock-outs. Then we tested the first integration site for the sKO cassette and faced an unexpected outcome. The PCR produced two fragments of different molecular weights instead of one. These results indicate unwanted genome rearrangement at the integration site of the first cassette.

We are planning to repeat the transfection of dKO cassette into sKO cells. If this transfection is unsuccessful again, we will change our knock-out strategy for TbIF1.

The 5’ and 3’UTR regions flanking the first sKO cassette will be changed for regions further away from the cds, while the second cassette and its flanked regions will remain the same. Therefore, there will be no homology between the dKO cassette and the first replaced allele which should force the cell to incorporate the dKO cassette at the correct position in the genome. After creating the TbIF1 dKO cell line, the role of the TbIF1 during the *in vitro* differentiation will be examined. It will be very interesting to observe if epimastigotes or metacyclic-like cells are formed despite the lack of TbIF1 protein.

6. References

BASU, S., E. HORÁKOVÁ and J. LUKEŠ. Iron-associated biology of *Trypanosoma brucei*. Biochimica et Biophysica Acta (BBA) - General Subjects [online]. 2016, 1860(2), 363-370 [cit. 2018-03-14]. DOI: 10.1016/j.bbagen.2015.10.027. ISSN 03044165. Available from: http://linkinghub.elsevier.com/retrieve/pii/S0304416515002998

BRINGAUD, F., L. RIVIÈRE and V. COUSTOU. Energy metabolism of trypanosomatids: Adaptation to available carbon sources. Molecular and Biochemical Parasitology [online]. 2006, 149(1), 1-9 [cit. 2018-04-11]. DOI: 10.1016/j.molbiopara.2006.03.017. ISSN 01666851. Available from: http://linkinghub.elsevier.com/retrieve/pii/S0166685106001150

CAMPANELLA, M., E. CASSWELL, S. CHONG, Z. FARAH, M. R. WIECKOWSKI, A. Y. ABRAMOV, A. TINKER and M. R. DUCHEN. Regulation of Mitochondrial Structure and Function by the F1Fo-ATPase Inhibitor Protein, IF1. Cell Metabolism [online]. 2008, 8(1), 13-25 [cit. 2018-03-25]. DOI: 10.1016/j.cmet.2008.06.001. ISSN 15504131. Available from: http://linkinghub.elsevier.com/retrieve/pii/S1550413108001721

CROSS, G. A. M. Identification, purification and properties of clone-specific glycoprotein antigens constituting the surface coat of *Trypanosoma brucei*. Parasitology [online]. 1975, 71(03), 393- [cit. 2018-02-20]. DOI: 10.1017/S003118200004717X. ISSN 0031-1820. Available from: http://www.journals.cambridge.org/abstract_S003118200004717X

CROWE, J. S., J. D. BARRY, A. G. LUCKINS, C. A. ROSS and K. VICKERMAN. All metacyclic variable antigen types of *Trypanosoma congolense* identified using monoclonal antibodies. Nature [online]. 1983, 306(5941), 389-391 [cit. 2018-02-20]. DOI: 10.1038/306389a0. ISSN 0028-0836. Available from: http://www.nature.com/doifinder/10.1038/306389a0

CZICHOS, J., Ch. NONNENGAESSER and P. OVERATH. *Trypanosoma brucei*: cis-Aconitate and temperature reduction as triggers of synchronous transformation of bloodstream to procyclic trypomastigotes *in vitro*. Experimental Parasitology [online]. 1986, 62(2), 283-291 [cit. 2018-03-14]. DOI: 10.1016/0014-4894(86)90033-0. ISSN 00144894. Available from: http://linkinghub.elsevier.com/retrieve/pii/0014489486900330

DYER, N. A., C. ROSE, N. O. EJEH and A. ACOSTA-SERRANO. Flying tryps: survival and maturation of trypanosomes in tsetse flies. Trends in Parasitology [online]. 2013, 29(4), 188-196 [cit. 2018-03-08]. DOI: 10.1016/j.pt.2013.02.003. ISSN 14714922. Available from: http://linkinghub.elsevier.com/retrieve/pii/S1471492213000238

FORMENTINI, L., M. SÁNCHEZ-ARAGÓ, L. SÁNCHEZ-CENIZO and J. M. CUEZVA. The Mitochondrial ATPase Inhibitory Factor 1 Triggers a ROS-Mediated Retrograde Prosurvival and Proliferative Response. Molecular Cell [online]. 2012, 45(6), 731-742 [cit. 2018-04-11]. DOI: 10.1016/j.molcel.2012.01.008. ISSN 10972765. Available from: http://linkinghub.elsevier.com/retrieve/pii/S1097276512000494

FREIRE, A. C. Guimarães, C. L. ALVES, G. R. GOES, B. C. RESENDE, N. S. MORETTI, V. S. NUNES, P. H. N. AGUIAR, E. B. TAHARA, G. R. FRANCO, A. M. MACEDO, S. D. J. PENA, F. R. GADELHA, A. A. GUARNERI, S. SCHENKMAN, L. Q. VIERA and C. R. MACHADO. Catalase expression impairs oxidative stress-mediated signalling in *Trypanosoma cruzi*. Parasitology [online]. 2017, 144(11), 1498-1510 [cit. 2018-03-14]. DOI: 10.1017/S0031182017001044. ISSN 0031-1820. Available from: https://www.cambridge.org/core/product/identifier/S0031182017001044/type/journal_article

FURGER, A., N. SCHÜRCH, U. KURATH and I. RODITI. Elements in the 3'Untranslated Region of Procyclin mRNA Regulate Expression in Insect Forms of *Trypanosoma brucei* by Modulating RNA Stability and Translation. Molecular and cellular biology [online]. American Society for Microbiology, 1997, 1997, 17(8), 4372–4380 [cit. 2018-03-24]. Available from: https://www.ncbi.nlm.nih.gov/pmc/articles/PMC232291/pdf/174372.pdf

GARCÍA-BERMÚDEZ, J. and J. M. CUEZVA. The ATPase Inhibitory Factor 1 (IF1): A master regulator of energy metabolism and of cell survival. Biochimica et Biophysica Acta (BBA) - Bioenergetics [online]. 2016, 1857(8), 1167-1182 [cit. 2018-03-25]. DOI: 10.1016/j.bbabio.2016.02.004. ISSN 00052728. Available from: http://linkinghub.elsevier.com/retrieve/pii/S0005272816300238

GORMAN, C. M., L. F. MOFFAT and B. H. HOWARD. Recombinant Genomes Which Express Chloramphenicol Acetyltransferase in Mammalian Cells. Molecular and cellular biology [online]. American Society for Microbiology, 1982, 2(9), 1044-1051 [cit. 2018-04-08]. Available from: http://mcb.asm.org/content/2/9/1044.full.pdf

HAILE, S., Antonio M. ESTÉVEZ and C. CLAYTON. A role for the exosome in the *in vivo* degradation of unstable mRNAs. RNA [online]. 2003, 9(12), 1491-1501 [cit. 2018-04-10]. DOI: 10.1261/rna.5940703. ISSN 1355-8382. Available from: http://www.rnajournal.org/cgi/doi/10.1261/rna.5940703

IBRAHIM, S. F. and G. VAN DEN ENGH. Flow Cytometry and Cell Sorting. In: KUMAR, A., I. Y. GALAEV and B. MATTIASSON, ed. Cell Separation [online]. Berlin, Heidelberg: Springer Berlin Heidelberg, 2007, 2007-8-30, s. 19-39 [cit. 2018-02-07]. Advances in Biochemical Engineering/Biotechnology. DOI: 10.1007/10_2007_073. ISBN 978-3-540-75262-2. Available from: http://link.springer.com/10.1007/10_2007_073

JEFFERIES, D., P. TEBABI and E. PAYS. Transient Activity Assays of the *Trypanosoma brucei* Variant Surface Glycoprotein Gene Promoter: Control of Gene Expression at the Posttranscriptional Level. Molecular and Cellular Biology [online]. American Society for Microbiology, 1991, 1991, 11(1), 338-343 [cit. 2018-03-24]. Available: https://www.ncbi.nlm.nih.gov/pmc/articles/PMC359624/pdf/molcellb00136-0350.pdf

KOLEV, N. G., K. RAMEY-BUTLER, G. A. M. CROSS, E. ULLU and C. TSCHUDI. Developmental Progression to Infectivity in *Trypanosoma brucei* Triggered by an RNA-Binding Protein. Science [online]. 2012, 338(6112), 1352-1353 [cit. 2018-02-10]. DOI: 10.1126/science.1229641. ISSN 0036-8075. Available from: http://www.sciencemag.org/cgi/doi/10.1126/science.1229641

KOLEV, N. G., E. ULLU and C. TSCHUDI. The emerging role of RNA-binding proteins in the life cycle of *Trypanosoma brucei*. Cellular Microbiology [online]. 2014, 16(4), 482-489 [cit. 2018-02-10]. DOI: 10.1111/cmi.12268. ISSN 14625814. Available from: http://doi.wiley.com/10.1111/cmi.12268

LANGOUSIS, G. and K. L. HILL. Motility and more: the flagellum of *Trypanosoma brucei*. Nature Reviews Microbiology[online]. 2014, 12(7), 505-518 [cit. 2018-03-08]. DOI: 10.1038/nrmicro3274. ISSN 1740-1526. Available from: http://www.nature.com/articles/nrmicro3274

LODISH H., BERK A., ZIPURSKY S. L., et al. Molecular Cell Biology. 4th edition. New York: W. H. Freeman; 2000. Section 16.2, Electron Transport and Oxidative Phosphorylation. [cit. 2018-04-07]. Available from: https://www.ncbi.nlm.nih.gov/books/NBK21528/

MARCHETTI, M. A., C. TSCHUDI, H. KWON, S. L. WOLIN and E. ULLU. Import of proteins into the trypanosome nucleus and their distribution at karyokinesis. Journal of Cell Science. Great Britain: The Company of Biologists Limited 2000, [online]. 2000, 113, 899-906. Available from: http://jcs.biologists.org/content/joces/113/5/899.full.pdf

MAZET, M., P. MORAND, M. BIRAN, G. BOUYSSOU, P. COURTOIS, S. DAUlOUÈDE, Y. MILLERIOUX, J -M. FRANCONI, P. VINCENDEAU, P. MOREAU and F. BRINGAUD. Revisiting the Central Metabolism of the Bloodstream Forms of *Trypanosoma brucei*: Production of Acetate in the Mitochondrion Is Essential for Parasite Viability. PLoS Neglected Tropical Diseases [online]. 2013, 7(12), e2587-[cit. 2018-04-07]. DOI: 10.1371/journal.pntd.0002587. ISSN 1935-2735. Available from: http://dx.plos.org/10.1371/journal.pntd.0002587

MITCHELL, P. Coupling of Phosphorylation to Electron and Hydrogen Transfer by a Chemi-Osmotic type of Mechanism. Nature [online]. 1961, 191(4784), 144-148 [cit. 2018-04-13]. DOI: 10.1038/191144a0. ISSN 0028-0836. Available from: http://www.nature.com/doifinder/10.1038/191144a0

MORRIS, L. M., C. A. KLANKE, S. A. LANG, F-Y. LIM and T. M. CROMBLEHOLME. TdTomato and EGFP identification in histological sections: insight and alternatives. Biotechnic & Histochemistry [online]. 2010, 85(6), 379-387 [cit. 2018-03-29]. DOI: 10.3109/10520290903504753. ISSN 1052-0295. Available from: http://www.tandfonline.com/doi/full/10.3109/10520290903504753

MUGO, E., C. CLAYTON and L. READ. Expression of the RNA-binding protein RBP10 promotes the bloodstream-form differentiation state in *Trypanosoma brucei*. PLOS Pathogens [online]. 2017, 13(8), e1006560- [cit. 2018-02-22]. DOI: 10.1371/journal.ppat.1006560. ISSN 1553-7374. Available from: http://dx.plos.org/10.1371/journal.ppat.1006560

PANICUCCI, B., O. GAHURA, A. ZÍKOVÁ and J. RAPER. *Trypanosoma brucei* TbIF1 inhibits the essential F1-ATPase in the infectious form of the parasite. PLOS Neglected Tropical Diseases [online]. 2017, 11(4), e0005552- [cit. 2018-03-25]. DOI: 10.1371/journal.pntd.0005552. ISSN 1935-2735. Available from: http://dx.plos.org/10.1371/journal.pntd.0005552

PREUßER, C., N. JAÉ and A. BINDEREIF. MRNA splicing in trypanosomes. International Journal of Medical Microbiology [online]. 2012, 302(4-5), 221-224 [cit. 2018-02-18]. DOI: 10.1016/j.ijmm.2012.07.004. ISSN 14384221. Available from: http://linkinghub.elsevier.com/retrieve/pii/S143842211200032X

PULLMAN, M. E. and G. C. MONROY. A Naturally Occurring Inhibitor of Mitochondrial Adenosine Triphosphatase. The Journal of biological chemistry [online]. USA, 1963, 238(11), 3762-3769 [cit. 2018-03-25]. Available from: http://www.jbc.org/content/238/11/3762.long

RHEE, S. G. Redox signaling: hydrogen peroxide as intracellular messenger. Experimental and molecular medicine [online]. 1999, 1999, 31(2), 53-59 [cit. 2018-03-25]. Available from: https://www.nature.com/articles/emm19999.pdf

RODITI, Is., M. CARRINGTON and M. TURNER. Expression of a polypeptide containing a dipeptide repeat is confined to the insect stage of *Trypanosoma brucei*. Nature [online]. 1987, 325(6101), 272-274 [cit. 2018-02-20]. DOI: 10.1038/325272a0. ISSN 0028-0836. Available from: http://www.nature.com/articles/325272a0

ROLDÁN, A., M. A. COMINI, M. CRISPO and R. L. KRAUTH-SIEGEL. Lipoamide dehydrogenase is essential for both bloodstream and procyclic *Trypanosoma brucei*. Molecular Microbiology [online]. 2011, 81(3), 623-639 [cit. 2018-03-13]. DOI: 10.1111/j.1365-2958.2011.07721.x. ISSN 0950382X. Available from: http://doi.wiley.com/10.1111/j.1365-2958.2011.07721.x

ROTUREAU, B., I. SUBOTA, J. BUISSON and P. BASTIN. A new asymmetric division contributes to the continuous production of infective trypanosomes in the tsetse fly. Development [online]. 2012, 139(10), 1842-1850 [cit. 2018-03-08]. DOI: 10.1242/dev.072611. ISSN 0950-1991. Available from: http://dev.biologists.org/cgi/doi/10.1242/dev.072611

SHARMA, R., E. GLUENZ, L. PEACOCK, W. GIBSON, K. GULL and M. CARRINGTON. The heart of darkness: growth and form of *Trypanosoma brucei* in the tsetse fly. Trends in Parasitology[online]. 2009, 25(11), 517-524 [cit. 2018-03-08]. DOI: 10.1016/j.pt.2009.08.001. ISSN 14714922. Available from: http://linkinghub.elsevier.com/retrieve/pii/S1471492209001810

SHANER, N. C., R. E. CAMPBELL, P. A. STEINBACH, B. N. G. GIEPMANS, A. E. PALMER and R. Y. TSIEN. Improved monomeric red, orange and yellow fluorescent proteins derived from *Discosoma* sp. red fluorescent protein. Nature Biotechnology [online]. 2004, 22(12), 1567-1572 [cit. 2018-02-07]. DOI: 10.1038/nbt1037. ISSN 1087-0156. Available from: http://www.nature.com/doifinder/10.1038/nbt1037

SHANER, N. C., P. A. STEINBACH and R. Y. TSIEN. A guide to choosing fluorescent proteins. Nature Methods [online]. 2005, 2(12), 905-909 [cit. 2018-03-29]. DOI: 10.1038/nmeth819. ISSN 1548-7091. Available from: http://www.nature.com/doifinder/10.1038/nmeth819

SMITH, T. K., F. BRINGAUD, D. P. NOLLAN and L. M. FIGUEIREDO. Metabolic reprogramming during the *Trypanosoma brucei* life cycle. F1000Research [online]. 2017, 2017, 6, Faculty Rev-683 [cit. 2018-03-26]. Available from: https://www.ncbi.nlm.nih.gov/pmc/articles/PMC5461901/

URWYLER, S., E. STUDER, C. K. RENGGLI and I. RODITI. A family of stage-specific alanine-rich proteins on the surface of epimastigote forms of *Trypanosoma brucei*. Molecular Microbiology [online]. 2007, 63(1), 218-228 [cit. 2018-02-20]. DOI: 10.1111/j.1365-2958.2006.05492.x. ISSN 0950-382X. Available from: http://doi.wiley.com/10.1111/j.1365-2958.2006.05492.x

VICKERMAN, K., L. TETLEY, K. A. K. HENDRY and C. M. R. TURNER. Biology of African trypanosomes in the tsetse fly. Biology of the Cell [online]. Paris: Elsevier, 1988, 1988, 64, 109-119 [cit. 2018-03-08]. Available from: https://www.ncbi.nlm.nih.gov/pubmed/3067793

WIRTZ, E., S. LEAL, C. OCHATT and G. A. M. CROSS. A tightly regulated inducible expression system for conditional gene knock-outs and dominant-negative genetics in *Trypanosoma brucei*. Molecular and Biochemical Parasitology [online]. 1999, 99(1), 89-101 [cit. 2018-04-10]. DOI: 10.1016/S0166-6851(99)00002-X. ISSN 01666851. Available from: http://linkinghub.elsevier.com/retrieve/pii/S01666851990000

WURST, M., B. SELIGER, B. A. JHA, C. KLEIN, R. QUEIROZ and C. CLAYTON. Expression of the RNA recognition motif protein RBP10 promotes a bloodstream-form transcript pattern in *Trypanosoma brucei*. Molecular Microbiology [online]. 2012, 83(5), 1048-1063 [cit. 2018-02-28]. DOI: 10.1111/j.1365-2958.2012.07988.x. ISSN 0950382X. Available from: http://doi.wiley.com/10.1111/j.1365-2958.2012.07988.x

Internet sources:

http://www.allelebiotech.com/mneongreen/

http://www.facs.ethz.ch/education.html